

An experimental and computational investigation of the site selective and lattice driven cycloaddition reactions of SNS^+ salts with 2,3-dichloro-5,6-dicyano-1,4-benzoquinone and 1,1,2,2-tetracyanoethylene: Accounting for experimental findings for SNS^+ cycloaddition reactions with other related multi cyano-containing compounds using DFT and VBT approaches

Andreas Decken ^a, H. Donald B. Jenkins ^b, Aaron Mailman ^a, Jack Passmore ^{a,*},
Konstantin V. Shuvaev ^a

^a Department of Chemistry, University of New Brunswick, Fredericton, NB, Canada E3B 6E2

^b Department of Chemistry, University of Warwick, Coventry CV4 7AL, United Kingdom

Received 19 April 2007; accepted 17 May 2007

Available online 2 June 2007

Dedicated to Professor Anthony J. Downs on the occasion of his 70th birthday

Abstract

Reaction of SNSSbF_6 and DDQ (2,3-dichloro-5,6-dicyano-1,4-benzoquinone (**1**)) in SO_2 solution in a 2:1 ratio afforded the dicycloaddition product $\mathbf{1}(\text{SNS})_2(\text{SbF}_6)_2 \cdot \text{SO}_2$ in 85% isolated yield. The dicycloaddition product $\mathbf{1}(\text{SNS})_2(\text{SbF}_6)_2 \cdot \text{SO}_2$ was fully characterized by IR, Raman, NMR, elemental analysis, and single crystal X-ray crystallography. The product of the site selective dicycloaddition of SNS^+ at the nitrile functionalities of **1** represents the first structurally characterized *ortho*-bis-1,3,2,4-dithiadiazolium salt which adopts a conformation that utilizes the intramolecular $\text{S}^{\delta+}-\text{O}^{\delta-}$ electrostatic interactions. The reaction of **1** and $\text{SNS}[\text{Al}(\text{OC}(\text{CF}_3)_4)]$ in a 1:1 ratio yielded only the monocycloaddition product $\mathbf{1}(\text{SNS})[\text{Al}(\text{OC}(\text{CF}_3)_3)_4]$ identified by multinuclear ^{13}C , ^{14}N , ^{19}F , ^{27}Al NMR in SO_2 solution. The assignment of the ^{13}C NMR of $\mathbf{1}(\text{SNS})^+$ in SO_2 solution, were supported by comparison of the calculated (MPW1PW91/6-31G*) ^{13}C NMR and experimental chemical shifts, and by comparison of the observed chemical shifts of the related $\mathbf{2}(\text{SNS})^+$ produced on reacting the mono-nitrile CDMQ (2-cyano-5,6-dichloro-3-methoxy-1,4-benzoquinone (**2**)) with SNS^+ (as the SbF_6^- salt). The reaction of SNSSbF_6 with TCNE (1,1,2,2-tetracyanoethylene (**3**)) gave the tri-cycloaddition product $\mathbf{3}(\text{SNS})_3(\text{SbF}_6)_3 \cdot \text{SO}_2$ (IR, Raman microscopy and X-ray crystallography) in 40% yield.

The energetics of the cycloaddition reactions of SNS^+ with **1–3** and other multifunctional unsaturated centers (e.g. $\text{HC}\equiv\text{C}-\text{CN}$, $\text{NC}-\text{CN}$, $\text{C}(\text{CN})_3^-$, *o,m,p*- $(\text{CN})_2\text{C}_6\text{H}_4$, 1,3,5- $(\text{NC})_3\text{C}_6\text{H}_3$, **4–10**, previously reported, see Chart 1), were estimated in the gas phase (MPW1PW91/6-31G*), solution (PBE0/6-311G*) and in the solid state by the ‘volume based thermodynamics’ (VBT) approach. The general thermodynamic trends associated with the stepwise cycloaddition of SNS^+ with multifunctional nitriles were established. The 1:1 cycloaddition products were calculated to be stable in the gas phase and solution, while in the solid state the larger lattice enthalpy of the 1:2 salt, relative to twice that of the 1:1 salt, favored the 1:2 cycloaddition product.

© 2007 Elsevier B.V. All rights reserved.

Keywords: 1,3,2,4-Dithiadiazolium; Symmetry allowed cycloaddition; Thermodynamics; DFT; VBT (volume-based thermodynamics); Calculated energetics; SNS^+ ; DDQ

* Corresponding author. Tel.: +1 506 4534821; fax: +1 506 4534981.

E-mail address: passmore@unb.ca (J. Passmore).

1. Introduction

The general utility of SNS^+ as a synthon in sulfur–nitrogen chemistry [1] has been advanced by the convenient large scale synthesis of SNSSbF_6 [2a] and recent preparation of $\text{SNS}[\text{Al}(\text{OC}(\text{CF}_3)_3)_4]$, which is soluble in CH_2Cl_2 [2b]. The quantitative, symmetry allowed cycloaddition chemistry of SNS^+ with a variety of relatively simple derivatives containing unsaturated centers (e.g., olefins, acetylenes and nitriles) has been extensively investigated [3]. While other routes to both dithiadiazolylum isomers (R-CNSNS^+ and R-CNSSN^+) are known [4,6b], the reaction of SNS^+ with a nitrile is essentially the only general, quantitative route to the 1,3,2,4-dithiadiazolylum isomer [3]. On reduction the R-CNSNS^+ gives the corresponding 7π R-CNSNS^\bullet radical, which is isolable in some cases [5–9a], but typically rearranges to the corresponding thermodynamically more stable 1,2,3,5-dithiadiazolyl radical isomer (R-CNSSN^\bullet) [5]. This has provided access to a variety of stable multiradicals, incorporating either one or both dithiadiazolyl isomers [6], from the corresponding multifunctional nitriles and the readily available soluble SNSMF_6 ($\text{M} = \text{As}, \text{Sb}$). The physical and electronic properties of these and related, stable sulfur–nitrogen radical heterocycles are of current interest [7].

Typically, the reaction of SNS^+ with compounds containing two or more nitriles results in the transformation of every nitrile group to a 1,3,2,4-dithiadiazolylum moiety [8], with the exception of K^+ [4] [9a] and $5(\text{SNS})^+$ [9b], Chart 1.

In the case of K^+ [4] all three stepwise cycloaddition products were isolated and characterized. More recently the structure of the monocycloaddition product of $11(\text{SNS})^+$ has been determined by X-ray crystallography. In addition, a thermodynamic explanation both in solution and the solid state, for the preference of the dicycloaddition products $11(\text{SNS})_2^{2+}$ and $12(\text{SNS})_2^{2+}$ from the reactions of SNSMF_6 ($\text{M} = \text{As}, \text{Sb}$) with **11** and **12**, respectively [10], has been presented. An example of the stepwise cycloaddition of SNSX ($\text{X} = \text{any anion}$) to any dinitrile dipolarophile, (**A**), is given in the general Born–Fajan–Haber enthalpy cycle in Fig. 1. The enthalpy of sublimation for the dipolarophile (**A**) varies according to differences in molecular weight (i.e., mp, T_{fus}) and van der Waal forces, while the gas-phase terms (ΔH_{g1} , ΔH_{g2}) follow a general trend. Typically, the magnitude and favorability of the overall gas-phase reaction ($\Delta H_{\text{gas-phase}}$) is determined by ΔH_{g1} (e.g., $\text{A}(\text{SNS})^+$), which is always more favorable than ΔH_{g2} , due to the Coulomb repulsions which result from the addition of a second positive charge (e.g., $\text{A}(\text{SNS})_2^{2+}$). The ionic strength term, I , for a 1:1 salt ($I = 1$) and a 1:2 salt ($I = 3$), govern the relative magnitude of the lattice enthalpy contribution in the solid state, according to Eq. (D) (see below), while the sum of the individual ion volumes is additive and variable, only depending on the size of the anion (e.g., AsF_6^- ($V = 0.110\text{nm}^3$) versus $\text{Al}(\text{OC}(\text{CF}_3)_3)_4^-$ ($V = 0.719\text{nm}^3$)). Hence, the lattice

enthalpy contribution for both a 1:1 and 1:2 salt decreases when the volume of the anion increases. Therefore, it has been suggested that a strategy to obtain the monocycloaddition product, as the predominate product, would be the use of an SNS^+ salt of a very large anion (i.e., $\text{Al}(\text{OC}(\text{CF}_3)_3)_4^-$), thereby reducing the lattice enthalpy gain of the second cycloaddition (e.g., $\Delta H_{\text{s2}} \leq \Delta H_{\text{s1}}$) [10].

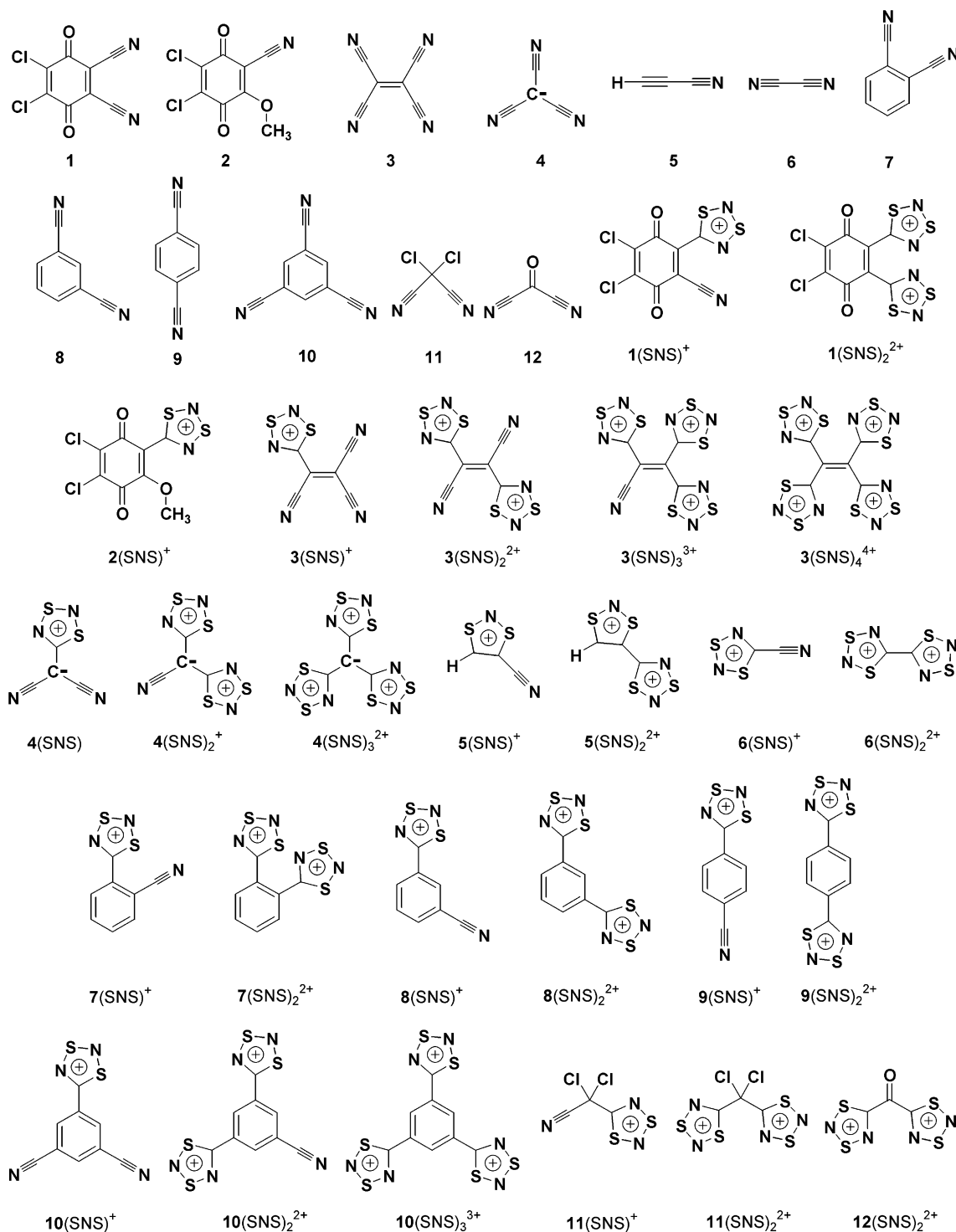
The isolation of the monocycloaddition products would provide a free nitrile group, which is a potential reactive site to introduce more diverse radical centers, (i.e. $-\text{CN} + \text{S}_3^{+\bullet} \rightarrow -\text{CNS}_3^{+\bullet}$). In addition, the free nitrile can act as a Lewis base in coordination to a transition metal center ($-\text{CN} \rightarrow \text{M}$) [11d] and as an additional link between neighboring molecules as a means of modifying the bulk properties in the solid state (e.g., potentially giving rise to ferromagnetism) [11a–c]. These possibilities have motivated us to explore the stepwise cycloaddition of SNS^+ with the strong electron acceptor **1** as a route to a new class of hybrid quinoidal–thiazyl systems [12]. The strong electron acceptors incorporating heavier main group elements, especially fused heterocyclic rings containing the quinoidal motif, are of central importance in the preparation of new conductive and magnetic materials, and have been an active research area in materials chemistry [13].

In this paper, we report the reaction of the dinitrile **1** with both SNSSbF_6 and $\text{SNS}[\text{Al}(\text{OC}(\text{CF}_3)_3)_4]$. Both the 1:1 and 1:2 cycloaddition products of **1** with SNSSbF_6 , $1(\text{SNS})^+$ and $1(\text{SNS})_2^{2+}$, respectively, were identified in SO_2 solution by multinuclear NMR. However, only the 1:2 cycloaddition product, $1(\text{SNS})_2^{2+}$, as the SbF_6^- salt, was isolated in the solid state. Conversely, the reaction of **1** with $\text{SNS}[\text{Al}(\text{OC}(\text{CF}_3)_3)_4]$ resulted only in the identification of the 1:1 cycloaddition product $1(\text{SNS})^+$ and unreacted starting materials in solution (multinuclear NMR) and solid state (IR).

The reaction of **3** with an excess of SNSSbF_6 in SO_2 solution yielded the 1:3 cycloaddition product, $3(\text{SNS})_3(\text{SbF}_6)_3$ salt, in 40% isolated yield. We account for the observations of these and related examples previously reported in the literature, based on our gas-phase and solution DFT calculations and the ‘volume based thermodynamics’ (VBT) approach [14] in the solid state, reported below.

2. Experimental

SNSSbF_6 [2a] and $\text{SNS}[\text{Al}(\text{OC}(\text{CF}_3)_3)_4]$ [2b] were prepared and purified according to the literature procedures, and the purity was confirmed by IR. DDQ (2,3-dichloro-5,6-dicyano-1,4-benzoquinone, **1**, Aldrich, 98%) was used as received. CDMQ (2-cyano-5,6-dichloro-3-methoxy-1,4-benzoquinone, **2**) was prepared and purified as described in the literature [15] (contained traces of DDQ, ^{13}C NMR) and dried under dynamic vacuum prior to use. TCNE (1,1,2,2-tetracyanoethylene, **3**, TCI America, 98%) was sublimed prior to use and the purity confirmed by IR. SO_2 (Sulfur dioxide, Liquid Air, 99.999%) was stored

Chart 1. Multifunctional nitriles and their corresponding 1:1 and 1:2 cycloaddition products with SNS^+ .

over CaH_2 for at least 24 h and freshly distilled prior to use. CH_2Cl_2 (spectroscopic grade) was refluxed over CaH_2 and freshly distilled prior to use. Solids were manipulated under a dry N_2 atmosphere in an MBraun drybox ($\text{O}_2 \leq 0.1$ ppm and $\text{H}_2\text{O} \leq 0.1$ ppm). Techniques and apparatus for carrying out reactions in SO_2 and CH_2Cl_2 in a closed greaseless Monel vacuum line, such that volatile

materials can be transferred quantitatively, have been described elsewhere [16].

FT-IR spectra were recorded on a Thermo Nicolet NEXUS 470 FT-IR (resolution 2 cm^{-1}) as Nujol mulls between CsI and KBr plates. Raman spectroscopy samples were sealed in dry melting point tubes and spectra were recorded on a Bruker IFS66 FT-IR equipped with a Bruker

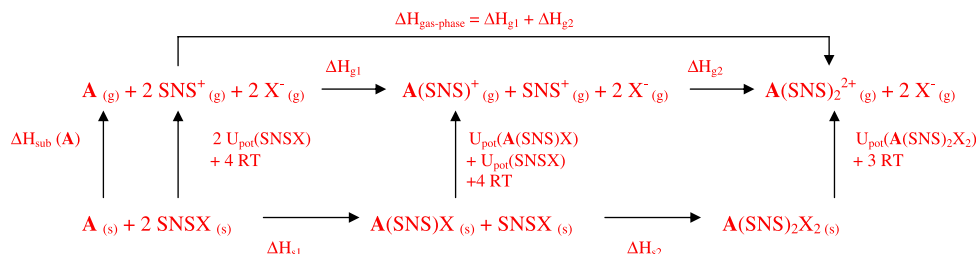


Fig. 1. A general Born–Fajan–Haber enthalpy cycle for the double cycloaddition of SNSX (X = any anion) and a dinitrile substrate (A).

FRA106 FT-Raman accessory using an Nd-YAG laser (emission wavelength: 1064 nm; maximum laser power: 300 mW). Data were collected in the backscattering mode (180° excitation, resolution 2 cm⁻¹). Raman microscopy was performed on a Renishaw inVia RE 08 microscope with enclosure using a HeNe laser (emission wavelength: 633 nm; maximum laser power: 17 mW) and a CCD detector. Data were collected using 20 scans from 3200–100 cm⁻¹, resolution 4 cm⁻¹, and 10% laser power output. NMR spectra were recorded on a Varian 400 NMR spectrometer in 10 mm NMR tubes that were flame sealed and were externally referenced to TMS (¹³C), neat nitromethane (¹⁴N), CFC₃ in SO₂ (¹⁹F) and AlCl₃/D₂O (²⁷Al). Elemental analyses were carried out by Galbraith Laboratories, Inc., Knoxville, TN, USA.

Pyrex vessels of two types were employed throughout unless otherwise stated. Type A, incorporating a water cooled condenser with two 40 ml bulbs and closed by two Rotoflo (6 HK) Teflon in glass valves. Type B, incorporating two limbs (50 ml) separated by a 10 mm medium scintered frit and closed by two Rotoflo (6 HK) Teflon in glass valves. One of the limbs contained a Teflon coated magnetic stir bar. One piece 10 mm (o.d.) NMR tubes with 1/4 inch (6 mm, o.d.) Pyrex tube were connected to stainless steel Whitey® valves (1KS4) by Swagelok® compression fittings, using Teflon back and front ferrules. The Whitey® valves were attached directly to the vacuum line by 1/4 in. Monel tubing. The *in situ* NMR were obtained in a one piece 10 mm (o.d.) NMR tube, directly attached to the vessel by a 1/4 inch (6 mm) tube, and flame sealed. (See Figure S28 in supplemental material for diagrams of the reaction vessels).

2.1. Synthesis of $I(\text{SNS})_2(\text{SbF}_6)_2 \cdot \text{SO}_2$

Caution! Precautions should be taken to avoid explosion hazard when heating liquid SO₂ in a closed vessel (well ventilated fumehood, leather gloves, face shield, carefully built glass vessel).

A mixture of **1** (2.621 g, 11.55 mmol) and SNSSbF₆ (7.473 g, 23.81 mmol) were loaded to a vessel of Type A and heated in 20 ml of SO₂ at 50–60 °C for 7 days. (The liquid SO₂ was prevented from condensing to the cooler second bulb by closing the valve and isolating the condenser and reaction mixture, see Figure S28.) The resulting yellow–orange solution over a large quantity of orange crystals was concentrated by reducing solvent volume to

~10 ml by the removal of solvent under dynamic vacuum. The yellow–orange solution, containing the more soluble material was carefully decanted into bulb 2. The solvent was recondensed back into bulb 1 and the more soluble portion again decanted to bulb 2. This process was repeated twice more. The volatiles were removed under dynamic vacuum, leaving orange crystals in bulb 1 and a yellow–orange powder in bulb 2. The water contained in the condenser part of the vessel was rinsed with acetone and dried with a stream of dry N₂ before collecting the contents of the vessel in the dry box. The orange crystalline product (8.496 g, 10.0 mmol; 86% yield based on **1**, Eq. (1)) was collected and sealed in Pyrex sample tubes under N₂ and stored at –20 °C in order to avoid loss of any SO₂ of solvation. IR(CsI, nujol mull, cm⁻¹) with tentative assignments [17]: 3344vw (ν C=O overtone), 3314vw (ν C=O overtone), 1689 s (ν_{sym} C=O), 1667 s (ν_{asym} C=O), 1574 s (ν_{sym} C=C), 1416 m (ν C=N), 1321w (ν_{asym} SO₂), 1262s (ν_{asym} C–C), 1184s (ν_{sym} SO₂), 1086s (ν_{sym} C–C), 980w (ν [S–N]), 948w, 919w, 897w, 876w, 756m (ν [S–N]), 657vs (ν₃ SbF₆⁻), 588w, 574m, 539w (ν_{bend} SO₂), 487w, 457m, 447m (–CNSNS, ring bend), 421w, 377m (C=O bend), 287vs (ν₄ SbF₆⁻). FT-Raman (laser power, 68.8%, 500 scans): 1686(83) (ν_{sym} C=O), 1667(100) (ν_{asym} C=O), 1638(75), 1574(50) (ν_{sym} C=C), 1437(52), 1416(54) (ν C=N), 1321(30) (ν_{asym} SO₂), 1258(23) (ν_{asym} C–C), 1107(25) (ν_{sym} SO₂ or ν_{sym} C–C), 980(21), 897(26), 803(41), 720(20), 668(25), 648(67) (ν₁ SbF₆⁻), 576(46) (ν₂ SbF₆⁻), 486(31), 378(16), 332(20), 286(26) (ν₅ SbF₆⁻), 261(23), 199(21). *Anal. Calc.* for C₈Cl₂F₁₂N₄O₂S₄Sb₂: C, 11.24; N, 6.56; S, 15.01. Found: C, 11.17; N, 6.63; S, 14.72%. Actual spectra are given in the supplemental material (Figure S4, S7, S8). Assignments for the experimental and calculated IR and Raman frequencies are given in Table S5a in the supplemental material.

2.2. *In situ* multinuclear NMR study in SO₂ solution of the reaction of **1** and SNSSbF₆ in a 1:2 ratio

Similar to the reaction described in Section 2.1, a mixture of **1** (1.164 g, 5.13 mmol) and SNSSbF₆ (3.179, 10.13 mmol) was loaded to a vessel of Type A with a 10 mm (o.d.) NMR tube attached (See Figure S28). 20 ml of SO₂ was condensed, and the mixture heated at 50–60 °C for 4 days. A small portion (~4 ml) of the orange–brown solution, over an orange crystalline solid, was poured into the attached 10 mm NMR tube and flame

sealed. The orange crystalline solid was washed and collected in the drybox ($\mathbf{1}(\text{SNS})_2(\text{SbF}_6)_2\text{SO}_2$, IR) 3.516 g, 4.1 mmol, 81% yield; based on SNSSbF_6 , Eq. (1). ^{13}C NMR (100.6 MHz, SO_2 , r.t.); Obs. for $\mathbf{1}(\text{SNS})_2^{2+}$: δ 189.9, $-\text{CNSNS}$; 174.6, $-\text{C}=\text{O}$; 143.1, $-\text{C}-\text{Cl}$; 133.9, $-\text{C}(\text{CNSNS})$; Obs. for $\mathbf{1}(\text{SNS})^+$: δ 190.4, $-\text{CNSNS}$; 175.6, $-\text{C}=\text{O}$; 170.5, $-\text{C}=\text{O}$; 144.3, $\text{C}-\text{Cl}$; 141.7, $-\text{C}-\text{Cl}$; 136.3, $\text{C}-\text{CNSNS}$; 122.5, $-\text{C}-\text{CN}$; 111.4 $-\text{CN}$; Obs. for $\mathbf{1}$: δ 170.7, $-\text{C}=\text{O}$; 142.5, $\text{C}-\text{Cl}$; 128.2, $-\text{C}-\text{CN}$; 110.4, $-\text{CN}$ and several weak unassigned resonances; ^{14}N NMR (28.9 MHz, SO_2 , r.t.); Obs. for $\mathbf{1}(\text{SNS})_2^{2+}$: δ 20.0 ($\nu_{1/2} = 2876$ Hz), $-\text{CNSNS}$; -23.9 ($\nu_{1/2} = 2374$ Hz), $-\text{CNSNS}$; -95.5 ($\nu_{1/2} = 7$ Hz), SNS^+ ; and NH_4^+ δ -366 . The ^{14}N NMR peaks were assigned based on Ref. [18a]. Actual spectra are given in the supplemental material (Figure S19, S20 and Table S4). The calculated tentative assignments for the NMR of $\mathbf{1}(\text{SNS})_2(\text{SbF}_6)_2$ are tabulated for comparison.

2.3. Reaction of SNSSbF_6 with an excess of $\mathbf{1}$

SNSSbF_6 (0.425 g, 1.354 mmol) and $\mathbf{1}$ (0.611 g, 2.272 mmol) were placed in separate limbs of a Pyrex vessel (Type B, see Figure S28). CH_2Cl_2 (15 ml) and SO_2 (5 ml) was condensed on to $\mathbf{1}$ and SNSSbF_6 , respectively. All the solids dissolved on warming to room temperature giving a yellow solution in limb 1 (containing $\mathbf{1}$) and a yellow-brown solution in limb 2 (containing SNSSbF_6). The two solutions were mixed in limb 1 giving a dark orange solution and the mixture stirred for 12 h at room temperature. The resulting dark orange-brown solution over a bright yellow-orange solid was filtered to limb 2 and the volatiles were removed under dynamic vacuum leaving an orange-brown solid in limb 2. A small volume of fresh SO_2 (2 ml) was condensed on to the yellow-orange solid in limb 1. The mixture was warmed to room temperature and the yellow solution filtered to limb 2. This process was repeated twice more until the filtrate was orange. The volatiles were removed under dynamic vacuum. The orange solid (0.476 g, 0.6 mmol, 82% yield based on SNSSbF_6 , Eq. (1) in limb 1 was identified as the 1:2 cycloaddition product, $\mathbf{1}(\text{SNS})_2(\text{SbF}_6)_2$ [IR]. The orange brown solid in limb 2 (0.609 g) was mainly starting materials ($\mathbf{1}$ and SNSSbF_6), with a small amount of cycloaddition product. IR (CsI, nujol mull, cm^{-1}) with tentative assignments [17]: 2227w (ν CN, $\mathbf{1}$), 2193w (ν CN), 1690 m,sh ($\nu_{\text{sym}} \text{C}=\text{O}$, $\mathbf{1}$ or $\mathbf{1}(\text{SNS})_2^{2+}$), 1675s ($\nu_{\text{asym}} \text{C}=\text{O}$, $\mathbf{1}$ or $\mathbf{1}(\text{SNS})_2^{2+}$), 1498s,sh (SNS^+) [2a], 1305m,br, 1262s ($\nu_{\text{asym}} \text{C}-\text{C}$), 1183m ($\nu_{\text{sym}} \text{SO}_2$), 1087s ($\nu_{\text{sym}} \text{C}-\text{C}$), 975w, 919w, 897w, 876m, 846w, 800m, 761w (ν [S–N]), 657vs ($\nu_3 \text{SbF}_6^-$), 575m, 486w, 457m, 448m ($-\text{CNSNS}$, ring bend), 388s ($\text{C}=\text{O}$ bend), 290vs ($\nu_4 \text{SbF}_6^-$).

2.4. Reaction of $\mathbf{1}$ and $\text{SNS}[\text{Al}(\text{OC}(\text{CF}_3)_3)_4]$ in a 1:1 ratio in SO_2 solution

A mixture $\mathbf{1}$ (0.517 g, 2.28 mmol) and $\text{SNS}[\text{Al}(\text{OC}(\text{CF}_3)_3)_4]$ (2.195 g, 2.10 mmol) in 10 ml of SO_2 was stirred for 7

days in a Pyrex vessel of Type B (see Figure S28), giving a brown solution over a small amount of very fine white solid. The brown solution was filtered and the volatiles removed under dynamic vacuum yielding an orange brown solid, collected (2.586 g, 97% based on $\text{SNS}[\text{Al}(\text{OC}(\text{CF}_3)_3)_4]$ and Eq. (2) in the drybox. IR (CsI, nujol, cm^{-1}) with tentative assignments [17] for $\mathbf{1}(\text{SNS})^+$: 3345vw ($\text{C}=\text{O}$ overtone), 3324vw ($\text{C}=\text{O}$ overtone), 2235w (ν CN), 1694 m,sh ($\nu_{\text{sym}} \text{C}=\text{O}$), 1675s ($\nu_{\text{asym}} \text{C}=\text{O}$), 1556s ($\nu_{\text{sym}} \text{C}=\text{C}$), 1095m (ν C–C str), 1043w, 916w (ν [S–N]), 897w (ring bend), 871w, 845m (ν [S–N]), 727s, 696m,sh (ring bend), 669m (ring deformation), 561m (ring bend), 446s ($-\text{CNSNS}$ ring bend), 377m ($\text{C}=\text{O}$ bend), 316w. The assignment of the frequencies for the anion $\text{Al}(\text{OC}(\text{CF}_3)_3)_4^-$ were identical with those reported for $\text{H}(\text{OEt})_2[\text{Al}(\text{OC}(\text{CF}_3)_3)_4]$ [17]. For comparison, the IR of $\mathbf{1}$ was obtained (Nujol mull, KBr, cm^{-1}): 3340vw ($\text{C}=\text{O}$ overtone), 3327vw ($\text{C}=\text{O}$ overtone), 2247w (ν CN), 2233w (ν CN), 1695m,sh (ν C=O), 1690m, sh, 1673s (ν C=O), 1554s (ν C=C), 1305w, 1269m, 1253m,sh, 1217w, 1174s, 1069w, 1009w, 958w, 932w, 897m, 802m, 653m,br, 457s, 376w. See supplemental material for actual spectra (Figure S1, S6) and IR frequency assignments (Table S5).

2.5. Multinuclear NMR study of the reaction of $\mathbf{1}$ and $\text{SNS}[\text{Al}(\text{OC}(\text{CF}_3)_3)_4]$ in a 1:1 ratio in SO_2 solution

In a sealed 10 mm o.d. Pyrex NMR tube, 0.584 g of the orange-brown solid was redissolved (Section 2.2) in SO_2 (5 ml). The NMR tube was inserted into a water cooled metal reflux condenser and gently heated at 40–50 °C. ^{14}N NMR spectrum indicated that the reaction was incomplete (δ -95 ppm, $\nu_{1/2} = 7$ Hz, SNS^+ [16a] after 4 days). The multinuclear NMR $\{^{13}\text{C}, ^{14}\text{N}, ^{19}\text{F}, ^{27}\text{Al}\}$ was periodically monitored at room temperature. After 16 days it appeared that not all the SNS^+ had reacted (^{14}N NMR). ^{13}C NMR (100.6 MHz, SO_2 , r.t.); Obs. for $\mathbf{1}(\text{SNS})^+$: δ 191.1, $-\text{CNSNS}$; 176.3, $-\text{C}=\text{O}$; 171.1, $-\text{C}=\text{O}$; 171.0, $-\text{C}=\text{O}$, $\mathbf{1}$; 145.3, $\text{C}-\text{Cl}$; 142.9, $\text{C}-\text{Cl}$, $\mathbf{1}$; 142.2, $-\text{C}-\text{Cl}$; 135.9, $\text{C}-\text{CNSNS}$; 128.4, $-\text{C}-\text{CN}$; 110.5, $-\text{CN}$, $\mathbf{1}$ and for the anion $\text{Al}(\text{OC}(\text{CF}_3)_3)_4^-$ δ 122.2 (q, CF_3 , $J^1_{\text{C}-\text{F}} = 292$ Hz) and δ 79.9 (br, $\text{C}(\text{CF}_3)_3$); ^{14}N NMR (28.9 MHz, SO_2 , r.t.): δ 23.5 ($\nu_{1/2} = 921$ Hz), $-\text{CNSNS}$, -33.3 ($\nu_{1/2} = 691$ Hz), $-\text{CNSNS}$, -95.3 ($\nu_{1/2} = 626$ Hz), $-\text{CN}$, plus a superimposed peak for SNS^+ δ -95); ^{19}F NMR (376.3 MHz, SO_2 , r.t.): δ -73.9 [s, CF_3], -73.2 and -74.2 are from small amount of decomposition of $[\text{Al}^-]$; ^{27}Al NMR (104.2 MHz, SO_2 , r.t.): δ 36.8 $[\text{Al}^-]$. ($[\text{Al}^-] = \text{Al}(\text{OC}(\text{CF}_3)_3)_4^-$) [2b]. Actual spectra are given in the supplemental (Figure S23–S26) and observed (calculated) ^{13}C NMR chemical shifts are given in Table S4.

2.5.1. Reaction of $\mathbf{3}$ and SNSSbF_6 in 1:4 ratio in SO_2 solution

10 ml of SO_2 was condensed onto a mixture of $\mathbf{3}$ (0.322 g, 2.53 mmol) and SNSSbF_6 (3.160 g, 10.06 mmol)

at $-196\text{ }^{\circ}\text{C}$ in a Pyrex vessel of type A. A light yellow-brown solution over a white solid at room temperature was heated under reflux at $50\text{--}60\text{ }^{\circ}\text{C}$ for 12 days giving a white-grey solid under a yellow-brown solution on cooling to room temperature. The solubles were decanted into bulb 2 and the white-grey solid washed twice ($\sim 2\text{ ml}$ of SO_2) until the filtrate were colorless. The volatiles were removed under dynamic vacuum giving a white-grey insoluble solid (2.45 g) in bulb 1 and the more soluble yellow-brown solid (0.936 g) in bulb 2. IR of the insoluble white-grey solid (CsI, nujol, cm^{-1}): 2279 m ($\nu\text{ CN}$), 2222w ($\nu\text{ CN}$), 1305w, 1166s ($\nu\text{ C=C}$), 1121w, 1099w, 966w, 948w, 919w, 889w, 851w, 812w, 773w, 650vs ($\nu_3\text{SbF}_6^-$), 576m, 560m, 554m, 293s ($\nu_4\text{SbF}_6^-$). The IR spectrum of the soluble fraction indicated the presence of unreacted SNSSbF₆ (Nujol mull, KBr, cm^{-1}): 1498s, sh (SNS⁺) [2a], 657vs ($\nu_3\text{SbF}_6^-$) and an unidentified cycloaddition product: 2273w, 2187w, 1329s, 1291 m, 1152w, 1082w, 1036w, 1018w, 962w, 936w, 889w, 495w, 448w, 388m. For comparison the IR spectrum of **3** (Figure S3) was obtained (Nujol mull, CsI, cm^{-1}): 2261m ($\nu\text{ CN}$), 2227w ($\nu\text{ CN}$), 1328s, 1154s ($\nu\text{ C=C}$), 1115w, 1087w, 958m, 934w, 916w, 804w, 555m, 579m, 428w.

2.5.2. Preparation and isolation of crystalline

$3(\text{SNS})_3(\text{SbF}_6)_3 \cdot \text{SO}_2$

3 (0.064 g, 0.5 mmol) and SNSSbF₆ (0.634 g, 2.02 mmol) were dissolved in 7 ml SO_2 and allowed to stand for 12 days at room temperature in one limb of Type B Pyrex vessel. The pale yellow solution over a clear, colorless crystalline solid was filtered into the limb 2. The crystalline solid in limb 1 was washed twice with two small portions of SO_2 and each time the more soluble portion filtered into limb 2. The volatiles were removed under dynamic vacuum giving a colorless crystalline $3(\text{SNS})_3(\text{SbF}_6)_3 \cdot \text{SO}_2$, (0.235 g, 44% yield based on **3**, Eq. (4)). The IR spectrum of crystalline $3(\text{SNS})_3(\text{SbF}_6)_3 \cdot \text{SO}_2$ (Nujol mull, CsI, cm^{-1}) and tentative assignments [17]: 2230w ($\nu\text{ CN}$), 1329s ($\nu\text{ C=N}$ or $\nu_{\text{asym}}\text{SO}_2$), 1253w, 1181w, 1151m ($\nu_{\text{sym}}\text{C-C}$ or $\nu_{\text{sym}}\text{SO}_2$), 1113w, 1081w, 1061vw, 1018vw, 976m ($\nu\text{ [S-N]}$), 957m ($\nu\text{ [S-N]}$), 919vw, 892m, 811s, 659vs ($\nu_3\text{SbF}_6^-$), 572m (SNS bend), 526m ($\nu_{\text{bend}}\text{SO}_2$), 478w, 438s ($\text{C}\equiv\text{N}$ bend.), 389w, 287vs ($\nu_4\text{SbF}_6^-$). Raman microscopy (laser power 10%, 20 scans): 2236(42) ($\nu\text{ CN}$), 1578(100) ($\nu\text{ C=C}$), 1444(41) ($\nu\text{ C=N}$, ring 2 and 3 (Fig. 4), 1396(43) ($\nu\text{ C=N}$, ring 1 (Fig. 4)), 1328(20), 1261(19), 1252(20), 1151(48), 1030(16), 974(15), 955(17), 924(27), 879(14), 808(17), 788(21), 714(14), 644(31) ($\nu_1\text{SbF}_6^-$), 582(24) (SNS bend or $\nu_2\text{SbF}_6^-$), 563(15), 522(10), 277(11) ($\nu_5\text{SbF}_6^-$). Actual spectra are given in Figure S3 and S9 in the supplemental material.

2.6. In situ multinuclear NMR study in SO_2 solution of the reaction of **2** and SNSSbF₆ in a 1:2 ratio

A mixture of **2** (0.132 g, 0.569 mmol) and SNSSbF₆ (0.167 g, 0.532 mmol) in 7 ml of SO_2 was prepared in a

sealed Pyrex 10 mm o.d. NMR tube giving an orange solution over a bright yellow solid. Gentle agitation of the tube for 5 min resulted in a dark orange solution with no undissolved solid. The NMR spectra were obtained after 12 h ¹³C NMR (100.6 MHz, SO_2 , r.t.); Obs. (Calc. for **2**(SNS)⁺): δ 192.8 (190.8), -CNSNS; 177.3 (173.8) -C=O; 173.3 (168.6), -C=O; 162.5 (160.3), -COCH₃; 142.2 (155.6), -C-Cl; 141.7 (150.2);, -C-Cl; 113.7 (114.3), -C(CNSNS); 67.6 (73.2), -OCH₃; Several weak resonances observed for **2**, Obs. (Calc. for **2**): δ 174.1 (176.7), -C=O; 172.5 (172.8), -C=O; 163.5 (160.1), -C-OCH₃; 140.8 (151.4), -C-Cl; 132.1 (146.1), -C-Cl; 114.1 (109.7), -C-CN; not observed (104.4), -CN; 62.6 (67.2), -OCH₃; **1**, impurity in **2**; Obs. (Calc. for **1**): δ 171.0 (173.1), -C=O; 142.9 (150.0), -C-Cl; 128.4 (129.4), -C-CN; 110.5 (109.8), -CN; ¹⁴N NMR for **2**(SNS)⁺, (28.9 MHz, SO_2 , r.t.): δ 16.5 ($\nu_{1/2} = 4084\text{ Hz}$), -CNSNS; -49.0 ($\nu_{1/2} = 1373\text{ Hz}$), -CNSNS. Resonances for SNS⁺, δ -95; NH₄⁺, δ -366; one unassigned resonance, δ -218 ppm. See supplemental materials for actual spectra (Figure S17–18, **1** and Figure S21–22 for **2**(SNS)⁺) and Table S4 for comparison of observed (calculated) ¹³C NMR tensors and full assignments). IR spectrum of **2** (CsI, Nujol mull, cm^{-1}): 3387vw (C=O overtone), 3317vw (C=O overtone), 2227 m ($\nu\text{ CN}$), 1704s ($\nu_{\text{asym}}\text{C=O}$), 1662s ($\nu_{\text{sym}}\text{C=O}$), 1616s ($\nu_{\text{sym}}\text{C=C}$), 1583s ($\nu_{\text{asym}}\text{C=C}$), 1524w, 1333m, 1285w, 1265w, 1239s, 1187w, 1174m, 1102m, 980m, 883m, 806m, 765w, 732m, 668vw, 608w, 557w, 503w, 464w, 444w, 415w, 385w. See supplemental material for actual spectrum (Figure S2).

2.7. Crystal structure determinations

Suitable single crystals of **1**(SNS)₂(SbF₆)₂ · SO₂ and **3**(SNS)₃(SbF₆)₃ · SO₂ were obtained from SO₂ solutions. The SO₂ was removed under dynamic vacuum (with limited exposure of crystals to prolonged dynamic vacuum (5 min), since they are SO₂ solvates), and the crystals collected in the dry box. The suitable single crystals were coated with Paratone-N oil in a sample vial and mounted using a 20 μm cryoloop and frozen in the cold nitrogen stream of the goniometer. Data were collected on a Bruker AXS P4/Smart 1000 diffractometer using ω and θ scans with a scan width of 0.3° and 30 s exposure times. The detector distance was 5 cm for **1**(SNS)₂(SbF₆)₂ · SO₂ and 6 cm for **3**(SNS)₃(SbF₆)₃ · SO₂. In the case of **1**(SNS)₂(SbF₆)₂ · SO₂ the crystal was a twin and the orientation matrix for the major component determined [19a]. The data were reduced [19b] and corrected for absorption [19c]. The structures were solved by direct methods and all atoms refined anisotropically by full-matrix least squares on F^2 [20]. All figures illustrating crystal structures were prepared using the program DIAMOND [21]. Crystal structure refinement data for both **1**(SNS)₂(SbF₆)₂ · SO₂ and **3**(SNS)₃(SbF₆)₃ · SO₂ are given in Table 1.

Table 1
Crystal data and structure refinement

	$\mathbf{1}(\text{SNS})_2(\text{SbF}_6)_2 \cdot \text{SO}_2$	$\mathbf{3}(\text{SNS})_3(\text{SbF}_6)_3 \cdot \text{SO}_2$
Empirical formula	$\text{C}_8\text{Cl}_2\text{F}_{12}\text{N}_4\text{O}_6\text{S}_5\text{Sb}_2$	$\text{C}_6\text{F}_{18}\text{N}_7\text{O}_2\text{S}_7\text{Sb}_3$
Formula weight	918.829	1133.8
CCDC deposit no.	635254	635255
Temperature (K)	173	173
Wavelength (Å)	0.71073	0.71073
Crystal size (mm)	$0.60 \times 0.20 \times 0.15$	$0.45 \times 0.40 \times 0.25$
Color and habit	yellow, irregular	colorless, irregular
Crystal system	triclinic	monoclinic
Space group	$P\bar{1}(2)$	$P2(1)/n$
<i>a</i> (Å)	8.0329(8)	9.8155(8)
<i>b</i> (Å)	8.4438(9)	9.2621(7)
<i>c</i> (Å)	18.514(2)	30.212(2)
α (°)	90.331(2)	90
β (°)	97.467(2)	96.742(1)
γ (°)	109.349(2)	90
Volume (Å ³)	1173.19(9)	2727.64(5)
<i>Z</i>	2	4
<i>D</i> _{calc} (Mg/m ³)	2.60087	2.76078
Absorption coefficient (mm ⁻¹)	3.098	3.634
Reflections collected	7555	18235
Independent reflections	5012 [<i>R</i> _{int} = 0.0172]	6104 [<i>R</i> _{int} = 0.0221]
Index range	$-9 \leq h \leq 10,$ $-9 \leq k \leq 10,$ $-21 \leq l \leq 23$	$-12 \leq h \leq 12,$ $-11 \leq k \leq 11,$ $-38 \leq l \leq 39$
Data/parameter	5012/334	6104/388
Goodness-of-fit on <i>F</i> ²	1.163	1.173
Final <i>R</i> indices [<i>I</i> > 3σ(<i>I</i>)]	<i>R</i> ₁ = 0.0370, <i>wR</i> ₂ = 0.0969	<i>R</i> ₁ = 0.0275, <i>wR</i> ₂ = 0.0603
<i>R</i> indices (all data)	<i>R</i> ₁ = 0.0409, <i>wR</i> ₂ = 0.0991	<i>R</i> ₁ = 0.0304, <i>wR</i> ₂ = 0.0612
Largest difference peak and hole (e/Å)	1.532 and -1.926	1.161 and -0.628

2.8. Thermodynamic, electrostatic, and quantum chemical calculations

2.8.1. Quantum Chemical Calculations

All quantum-chemical calculations were carried out using the DFT methods as implemented in GAUSSIAN 03W suite of programmes [22]. The gas-phase calculations were carried out at the MPW1PW91 level [23a] with the 6-31G* basis set. Calculations are made for all the reactions listed in the second column of Tables 2 and 4 in which all the species listed are in the gas phase (e.g., Entry 1, Table 2, $\mathbf{1}(\text{g}) + \text{SNS}^+(\text{g}) \rightarrow \mathbf{1}(\text{SNS})^+(\text{g})$) and the numerical results for the enthalpy change for these gas phase reactions are displayed in column 3 of the tables. Entries in the fourth and fifth column refer to the corresponding reactions in the solid state (e.g. Entry 1, Table 2: for reaction: $\mathbf{1}(\text{s}) + (\text{SNS})\text{SbF}_6(\text{s}) \rightarrow \mathbf{1}(\text{SNS})(\text{SbF}_6)(\text{s})$, ΔH is listed in column 4 and for reaction: $\mathbf{1}(\text{s}) + (\text{SNS})[\text{Al}](\text{s}) \rightarrow \mathbf{1}(\text{SNS})[\text{Al}](\text{s})$, where $[\text{Al}] = \text{Al}(\text{OC}(\text{CF})_3)_4$ then ΔH is listed in column 5). Columns 6 and 7 (which include a ΔG value)

refer to the reaction $\mathbf{1}(\text{S}) + \text{SNS}^+(\text{S}) \rightarrow \mathbf{1}(\text{SNS})^+(\text{S})$, where (S) is solvent, taking place in (S) = SO₂ and (S) = CH₂Cl₂ respectively. In Table 4 Entry 1 corresponds to the reaction: $\text{K}^+[\mathbf{4}](\text{p}) + \text{SNSX}(\text{p}) \rightarrow \mathbf{4}(\text{SNS})(\text{p}) + \text{KX}(\text{p})$, where for column 3, X is absent and (p) = (g) representing the gaseous phase, in column 4, X = SbF₆ and (p) = (s); column 5, X = [Al] and in the final column the results for the reaction: $\text{K}^+[\mathbf{4}](\text{S}) + \text{SNS}^+(\text{S}) \rightarrow \mathbf{4}(\text{SNS})(\text{S}) + \text{K}^+(\text{S})$ are given for (S) = SO₂ as solvent.

The NMR tensors (at the MPW1PW91/6-31G* level of theory and 6-311G* basis set used for Cl and S atoms) were calculated by the GIAO method implemented in Gaussian 03W and referenced (¹³C, Benzene, *D*_{6h}) to obtain the calculated chemical shift, according to Eq. (A)

$$\delta(^{13}\text{C})|\text{Compound}| - \delta(^{13}\text{C})|\text{Benzene}| = \text{calculated chemical shift.} \quad (\text{A})$$

The referenced calculated chemical shifts were further correlated with the experimental chemical shift of benzene in SO₂ (¹³C NMR δ 129.2) [18b] to obtain the correlated chemical shift in SO₂ solution according to Eq. (B)

$$\text{Exp. } \delta(^{13}\text{C})\text{Benzene} - \text{calculated chemical shift} = \text{Correlated chemical shift.} \quad (\text{B})$$

Good agreement with the experimentally observed chemical shifts (± 5 ppm) was generally observed. The correlated ¹³C NMR chemical shifts for the C–Cl fragment were always found to be larger than those observed experimentally. This trend was relatively unchanged when using larger basis sets at the MPW1PW91 level of theory. The single point free energies in solution were calculated using a polarization continuum model (PCM) with the integral equation formalism (IEF) [24], employing the PBE0 DFT hybrid functional [23b,23c] and using the gas-phase optimized structures (confirmed as minima by the absence of imaginary frequencies) as inputs. The following parameters were used to describe the solvent SO₂: dielectric constant (*E*_{ps}) = 14.0, solvent radius (*R*_{solv}) = 2.021 Å, molar volume (*V*(SO₂)) = 46.75 Å³ = 0.0468 nm³ (used later in this paper), numeral density (ρ) = 0.01288 Å⁻³, density = 1.37027 g cm⁻³.

Rough electrostatic estimates of internal electrostatic potential energy were determined [25]¹, according to Eq. (C),

$$E_{\text{pot}} = [(333^* q_1^* q_2^*)/r]^* 4.184 \text{ kJ mol}^{-1} \quad (\text{C})$$

where the atoms were treated as point charges. The distances (*r*, Å) and Mulliken charges (Coulombs) were obtained from the gas-phase calculations (MPW1PW91/6-31G*).

¹ Only the major S^{δ+}–N^{δ-} interactions and the most apparent N^{δ-}–N^{δ-} interactions were determined as illustrated in Fig. 3. However, it was found that the S^{δ+}–N^{δ-} interactions are the most significant and a number of rotational isomers are envisioned.

Table 2
Calculated gas-phase and solution enthalpies (ΔH), solution Gibbs free energies (ΔG) and solid state estimates for **1**, **2** and **3** (Chart 1)

Entry	From Chart 1	Gas phase ^a	X ⁻ = [SbF ₆] ⁻ solid	X ⁻ = [Al] ⁻ solid	SO ₂ solution		CH ₂ Cl ₂ solution	
		ΔH	ΔH^b	ΔH^b	ΔH	ΔG^c	ΔH	ΔG^c
1	1 (g) + SNS ⁺ (g) → 1 (SNS) ⁺ (g) 1 (s) + SNSX (s) → 1 (SNS)X (s) (cycle A)	-159	+62	-21	-103	-63	-104	-55
2	1 (SNS) ⁺ (g) + SNS ⁺ (g) → 1 (SNS) ₂ ²⁺ (g) 1 (SNS)X (s) + SNSX (s) → 1 (SNS) ₂ (X) ₂ (s) (cycle A)	+109	-308	-218	-64	-19	-55	+1
3	1 (g) + 2SNS ⁺ (g) → 1 (SNS) ₂ ²⁺ (g) 1 (s) + 2 SNSX (s) → 1 (SNS) ₂ ²⁺ (X) ₂ (s) (cycle A)	-50	-246	-239	-167	-97	-159	-70
4	2 1 (SNS) ⁺ (g) → 1 (SNS) ₂ ²⁺ (g) + 1 (g) 2 1 (SNS)X (s) → 1 (SNS) ₂ X ₂ (s) + 1 (s) (cycle B)	+269	-366	-193	+39	+40	+49	+50
5	1 (g) + SNS ⁺ (g) → 1 -A ⁺ (g) (Scheme 1) 1 (s) + SNSX (g) → 1 -AX (s) (Scheme 1)	+27	+248	+165	+74	+15		
6	1 (g) + SNS ⁺ (g) → 1 -B ⁺ (g) (Scheme 1) 1 (s) + SNSX (g) → 1 -BX (s) (Scheme 1)	+23	+244	+161	+60	+1		
7	1 (g) + SNS ⁺ (g) → 1 -C ⁺ (g) (Scheme 1) 1 (s) + SNSX (g) → 1 -CX (s) (Scheme 1)	+41	+262	+179	+88	+25		
8	2 (g) + SNS ⁺ (g) → 2 (SNS) ⁺ (g)	-185	Sublimation enthalpy of 2 unknown	Sublimation enthalpy of 2 unknown	-106	-61		
	3 (g) + SNS ⁺ (g) → 3 (SNS) ⁺ (g) 3 (s) + SNSX (s) → 3 (SNS)X (s) (cycle C)	-100	+44	-7	-82	-46		
10	3 (SNS) ⁺ (g) + SNS ⁺ (g) → 3 (SNS) ₂ ²⁺ (g) ^d 3 (SNS)X (s) + SNSX (s) → 3 (SNS) ₂ (X) ₂ (s) (cycle C)	+118	-298	-216	-71	-30		
11	3 (SNS) ₂ ²⁺ (g) + SNS ⁺ (g) → 3 (SNS) ₃ ³⁺ (g)	+412	Lattice energies not available	Lattice energies not available	-117	-100		
12	3 (SNS) ₃ ³⁺ (g) + SNS ⁺ (g) → 3 (SNS) ₄ ⁴⁺ (g)	+630	Lattice energies not available	Lattice energies not available	+96	+72		
13	2 3 (SNS)X (s) → 3 (SNS) ₂ (X) ₂ (s) + 3 (s) (cycle D)	+218	-338	-206	+11	+8		

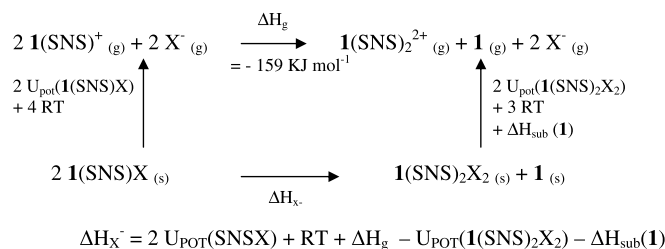
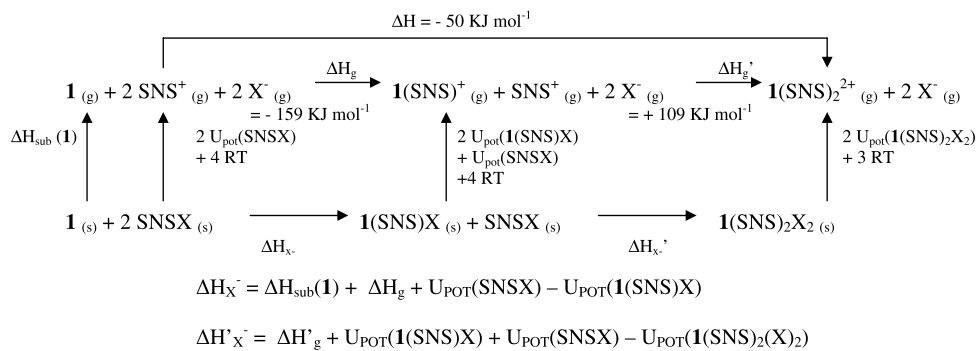
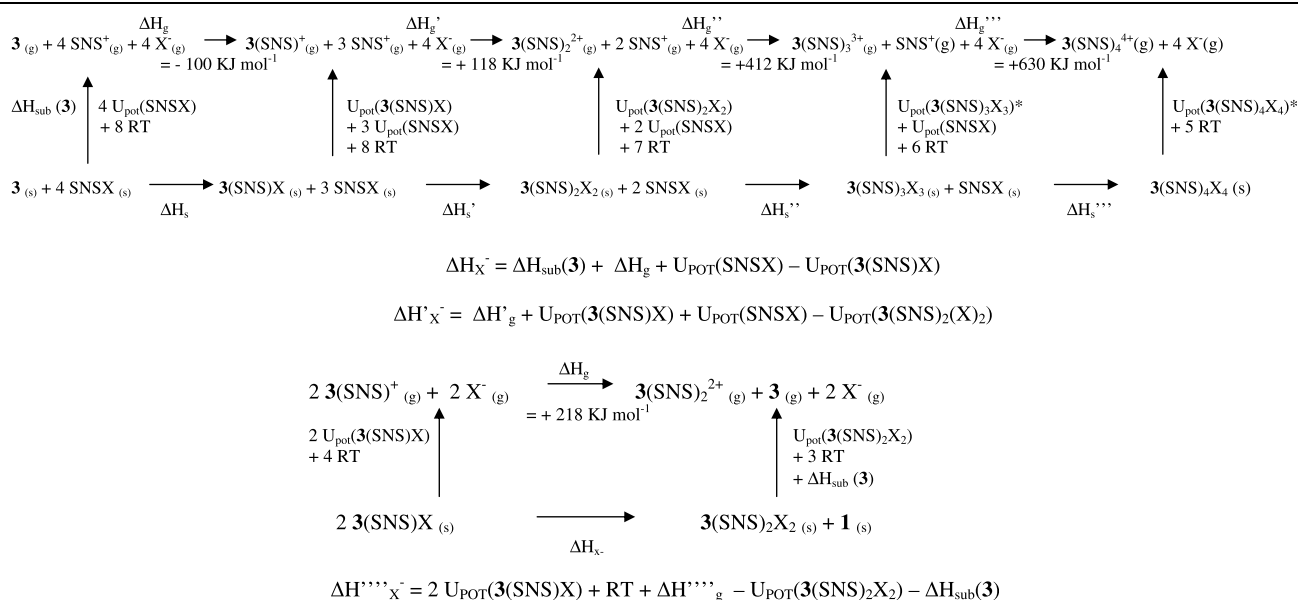


Table 2 (continued)



^a Includes zero point energy (ZPE) correction.

^b Calculated from appropriate Born–Haber cycles illustrated below, using the calculated gas phase values, RT terms, and the volume based thermodynamic (VBT) estimates of the lattice potential energies (see supplemental material for full details).

^c Including thermal correction to Gibbs free energy taken from the MPW1PW91/6-31G*(gas-phase) frequency calculations.

^d Three isomers are possible for the second cycloaddition of SNS⁺ with 3(SNS)⁺ with respect to the –CNSNS ring (trans, cis or vicinal) of which, the trans isomer (Chart 1) is the minimum in the gas-phase (MPW1PW/6-31G*).

2.9. VBT and volume calculations

The lattice potential energy (U_{pot}) of salts were estimated using the volume based thermodynamic (VBT) approach by Jenkins et al. [14a] according to Eq. (D),

$$U_{\text{pot}} = 2I(\alpha V_m^{-1/3} + \beta) \quad (\text{D})$$

For 1:1 salts (monocation and monoanion), $\alpha/\text{kJ mol}^{-1} \text{ nm} = 117.3$, $\beta/\text{kJ mol}^{-1} = 51.9$, $I = 1$; For 1:2 salts (dication and two monoanions), $\alpha/\text{kJ mol}^{-1} \text{ nm} = 133.5$, $\beta/\text{kJ mol}^{-1} = 60.9$, $I = 3$. Small errors in the volume are mitigated by this method (i.e., $U_{\text{pot}} \propto V^{-1/3}$), hence the small contribution from the volume of the SO_2 , $V(\text{SO}_2)$ of solvation to the total volume in both $\mathbf{1}(\text{SNS})_2(\text{SbF}_6)_2 \cdot \text{SO}_2$ and $\mathbf{3}(\text{SNS})_3(\text{SbF}_6)_3 \cdot \text{SO}_2$ are minimal (although using the volume above could be taken into account). The lattice energy, on incorporation into the traditional Born–Fajans–Haber enthalpy cycle requires correction to an enthalpy term as described by Jenkins [14e,14f] by the inclusion of the appropriate number of RT terms, determined by the stoichiometry and the nature (geometry) of the complex ions which are involved in the lattice energy stage(s).

Based on X-ray structural determinations, an estimate of a formula unit volume, V_m (i.e., $V_m = V_{\text{cell}}/Z$) can be determined. Hence, for a given formula unit volume, V_m , of a given salt, M_pX_q , the individual ion volume components can be calculated (i.e., $V_m(\text{M}_p\text{X}_q) \approx p(V(\text{M}^{q+}) + q(V(\text{X}^{p-})))$ [14b]. Here we obtain the formula unit volume

of $\mathbf{1}(\text{SNS})_2(\text{SbF}_6)_2 \cdot \text{SO}_2$, as $V_m = 1.17319/2 = 0.587 \text{ nm}^3$ from the X-ray crystal structure (Table 1). As a result of the work of Hofmann [14g], who has, on the basis of analysis of the Cambridge Structural Database (CSD) listed the average volumes assignable to various atoms within crystal structures and thus provides a means of estimating volumes of materials. Accordingly from summation of Hofmann's atom volume data we can estimate that $V(\mathbf{1}(\text{SNS})_2(\text{SbF}_6)_2 \cdot \text{SO}_2) = V(\text{C}_8\text{Cl}_2\text{F}_{12}\text{N}_4\text{O}_6\text{S}_5\text{Sb}_2) = 0.634 \text{ nm}^3$ which is within 0.047 nm^3 of the volume as determined by X-ray analysis of the actual compound.

The volume of the SbF_6^- anion is $V(\text{SbF}_6^-) = 0.121 \text{ nm}^3$ [14a], therefore since: $V(\mathbf{1}(\text{SNS})_2^{2+}) \approx V(\mathbf{1}(\text{SNS})_2(\text{SbF}_6)_2 \cdot \text{SO}_2) - 2V(\text{SbF}_6^-) - V(\text{SO}_2) = 0.587 - 2(0.121) - 0.047 = 0.298 \text{ nm}^3$. Alternatively using Hofmann's data we can estimate that: $V(\mathbf{1}(\text{SNS})_2^{2+}) \approx V(\text{C}_8\text{O}_2\text{N}_4\text{S}_4\text{Cl}_2) = 0.332 \text{ nm}^3$. The two values average to $V(\mathbf{1}(\text{SNS})_2^{2+}) \approx 0.315 \text{ nm}^3$. Since $V(\text{SNS})^+ = 0.060 \pm 0.009 \text{ nm}^3$ and $V(\mathbf{1}(\text{SNS})_2^{2+}) = V(\mathbf{1}(\text{SNS})^+) + V(\text{SNS})^+$ we can now estimate $V(\mathbf{1}(\text{SNS})_2^{2+}) \approx 0.315 + 0.060 = 0.375 \text{ nm}^3$.

Also from the crystallographic data presented in Table 1 it is determined that: $V(\mathbf{3}(\text{SNS})_3(\text{SbF}_6)_3 \cdot \text{SO}_2) = 2.72764/4 = 0.682 \text{ nm}^3$ (which matches the Hofmann data which gives $V(\mathbf{3}(\text{SNS})_3(\text{SbF}_6)_3 \cdot \text{SO}_2) \approx V(\text{C}_6\text{F}_{18}\text{N}_7\text{O}_2\text{S}_7\text{Sb}_3) = 0.710 \text{ nm}^3$, only 0.028 nm^3 different than our experimental result). Since: $V(\mathbf{3}(\text{SNS})_3^{3+}) \approx V(\mathbf{3}(\text{SNS})_3(\text{SbF}_6)_3 \cdot \text{SO}_2) - 3V(\text{SbF}_6^-) - V(\text{SO}_2) = 0.682 - 3(0.121) - 0.047 = 0.272 \text{ nm}^3$. Alternatively using Hofmann data we can estimate that: $V(\mathbf{3}(\text{SNS})_3^{3+}) \approx V(\text{C}_6\text{N}_7\text{S}_6) = 0.317 \text{ nm}^3$, which leads

to an average: $V(\mathbf{3}(\text{SNS})_3^{3+}) \approx 0.295 \text{ nm}^3$. Also since: $V(\mathbf{3}(\text{SNS})_2^{2+}) \approx V(\mathbf{3}(\text{SNS})_3^{3+}) - V(\text{SNS}^+)$ and $V(\mathbf{3}(\text{SNS})^+) \approx V(\mathbf{3}(\text{SNS})_2^{2+}) - V(\text{SNS}^+)$ then the volumes of the ions $V(\mathbf{3}(\text{SNS})_x^{x+})$ can be estimated to be 0.235 ($\mathbf{3}(\text{SNS})_2^{2+}$) and 0.175 nm^3 ($\mathbf{3}(\text{SNS})^+$) respectively. In general for any \mathbf{N} (Chart 1):

$$\begin{aligned} V(\mathbf{N}(\text{SNS})_{n+1}^{(n+1)+}) - V(\mathbf{N}(\text{SNS})_n^{n+}) &\approx V(\text{SNS}^+) \\ &= 0.060 \text{ nm}^3. \end{aligned} \quad (\text{E})$$

In this paper we also consider salts containing the anion $\text{Al}(\text{OC}(\text{CF}_3)_4)^-$ whose volume can be estimated in various ways. Firstly it could be estimated using Hofmann volumes, whereupon $V(\text{Al}(\text{OC}(\text{CF}_3)_4)^-) \approx V[\text{Al}] = V(\text{AlO}_4\text{C}_{16}\text{F}_{36}) = 0.709 \text{ nm}^3$. Alternatively referring to the study mentioned in the supplementary material included with reference [14b] where we estimated $V(\text{NO}(\text{Al}(\text{OC}(\text{CF}_3)_2\text{Ph})_4) = 0.9825 \text{ nm}^3$ we can approximate that: $V(\text{Al}(\text{OC}(\text{CF}_3)_4)^-) \approx V[\text{Al}] = V(\text{NO}(\text{Al}(\text{OC}(\text{CF}_3)_2\text{Ph})_4) - V(\text{NO}^+) - 20V(\text{C}) + 12V(\text{F}) - 20V(\text{H}) = 0.728 \text{ nm}^3$, averaging to give $V(\text{Al}(\text{OC}(\text{CF}_3)_4)^-) = 0.719 \text{ nm}^3$. Combining this volume with, for example, the value $V(\mathbf{1}(\text{SNS})_2^{2+}) = 0.375 \text{ nm}^3$ estimated above we can then (by additivity) estimate.

$V(\mathbf{1}(\text{SNS})_2(\text{Al}(\text{OC}(\text{CF}_3)_4)_2) = 0.375 + 2(0.719) = 1.813 \text{ nm}^3$. Using Eq. (D) for 1:2 salt (one dication and two monoanions, for which $I = 3$) we obtain the lattice potential energy for $\mathbf{1}(\text{SNS})_2(\text{Al}(\text{OC}(\text{CF}_3)_4)_2$ as 1022 kJ mol^{-1} . $U_{\text{pot}}(\mathbf{1}(\text{SNS})_2(\text{SbF}_6)_2)$ is calculated using $V(\mathbf{1}(\text{SNS})_2(\text{SbF}_6)_2) = [V(\mathbf{1}(\text{SNS})_2(\text{SbF}_6)_2 \cdot \text{SO}_2) - V(\text{SO}_2)] = 0.587 - 0.047 = 0.540 \text{ nm}^3$ in Eq. (D) taking the ionic strength factor to be $I = 1/2[1 \cdot (2)^2 + 2 \cdot (1)^2] = 3$ and giving 1349 kJ mol^{-1} . $V(\mathbf{1}(\text{SNS})_2(\text{SbF}_6)_2)$ is close to the Hofmann estimate $V(\text{C}_8\text{Cl}_2\text{O}_2\text{N}_4\text{S}_2\text{Sb}_2\text{F}_{12}) = 0.513 \text{ nm}^3$.

Unknown formula unit volumes, V_m , for ionic salts, can hence be estimated from volumes of analogous salts that have the same chemical formula and identical charge states (i.e., lattice ionic strength factors, I , Eq. (D) [14c] or using Hofmann's volumes [14g] for the ions $\mathbf{N}(\text{SNS})_n^{n+}$.

The experimental sublimation energy of a compound related to **1**, chloranil (2,3,5,6-tetrachloro-1,4-benzoquinone), is 98.7 kJ mol^{-1} [26]. From our comparison of related compounds, we estimate the replacement of two chloro- substituents by two cyano- substituents (see Table S1a and S1b in supplemental material for full details) in chloranil provides an enthalpy of sublimation for **1** as $110\text{--}120 \text{ kJ mol}^{-1}$.² This is expected to be higher than chloranil, since **1** has a larger dipole moment (sub-

limation enthalpy is dependent upon the strength of electrostatic interactions, dispersion forces, and dipole-dipole interactions). Accordingly we take $\Delta H_{\text{sub}}(\mathbf{1}) \approx 115 \text{ kJ mol}^{-1}$.

3. Results and discussion

3.1. Cycloaddition chemistry of SNS^+ with **1**

The cycloaddition reaction of SNS^+ , as the SbF_6^- salt, with the nitrile functionalities of **1** (2:1 stoichiometry) in refluxing SO_2 solution gave the corresponding dicycloaddition product, $\mathbf{1}(\text{SNS})_2(\text{SbF}_6)_2 \cdot \text{SO}_2$ in high yield (85%, based on SNSSbF_6 and Eq. (1)). The dicycloaddition products are less soluble than the 1:1 salts and readily precipitate or crystallize from SO_2 solution. The preparation of the mono-cycloaddition product, $\mathbf{1}(\text{SNS})(\text{SbF}_6)$, in a mixture of SO_2 and CH_2Cl_2 was attempted, expecting the 1:1 product to be less soluble (CH_2Cl_2 has a lower dielectric constant than SO_2), but the dicycloaddition product $\mathbf{1}(\text{SNS})_2(\text{SbF}_6)_2 \cdot \text{SO}_2$ was obtained instead (IR, 82% yield) [27]. The mono-cycloaddition product, $\mathbf{1}(\text{SNS})(\text{SbF}_6)$ was not identified in the solid state by IR. However, an *in situ* reaction (Eq. (1)) of two equivalents of SNSSbF_6 and **1** in SO_2 solution (^{13}C , ^{14}N NMR spectra are given in Figure S19 and S20, respectively) gave a mixture of both 1:1 and 1:2 cycloaddition products after 4 days (ca. 2:1 ratio of $\mathbf{1}(\text{SNS})_2^{2+}$ (^{13}C obs.(calc. for $\mathbf{1}(\text{SNS})_2^{2+}$): 189.9 (191.4), 174.6 (176.1), 143.1 (155.8), 133.9 (136.6) and $\mathbf{1}(\text{SNS})^+$ (^{13}C obs. (calc. for $\mathbf{1}(\text{SNS})^+$): 190.4 (193.1), 175.6 (178.7), 170.5 (171.7), 144.3 (156.6), 142.5 (149.6), 136.3 (134.6), 122.5 (125.3), ~ 111 (111.2), respectively). The relative ratio of $\mathbf{1}(\text{SNS})^+$ and $\mathbf{1}(\text{SNS})_2^{2+}$ cycloaddition products was

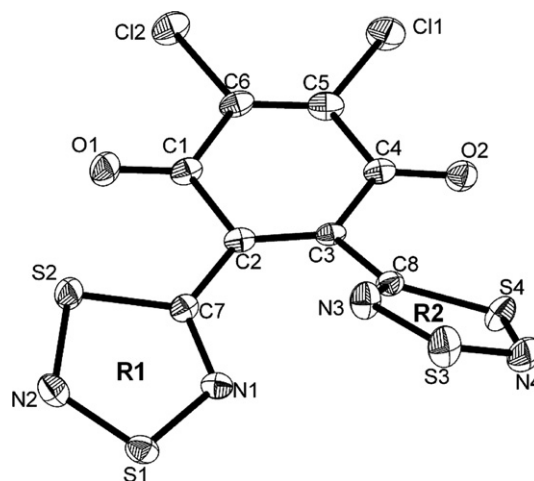


Fig. 2. Structure of $\mathbf{1}(\text{SNS})_2^{2+}$. Ellipsoids are drawn at the 50% probability level. Selected bond lengths (Å) and angles (°): C1–O1 1.209(5), C4–O2 1.212(5), C2–C3 1.349(5), R1: C2–C7 1.476(6), C7–N1 1.308(6), N1–S1 1.612(4), S1–N2 1.580(4), S2–N2 1.611(5), C7–S2 1.745(4); R2: C3–C8 1.471(5), C8–N3 1.308(5), S3–N3 1.608(4), S3–N4 1.590(4), S4–N4 1.600(4), C8–S4 1.739(4). Selected angles (°): O1–C1–C2 120.4(4), O2–C4–C3 119.7(3), C2–C3–C8 125.6(4), C3–C2–C7 126.0(3), and selected dihedral angles (°): C7–C2–C3–C8 11.8(7), O1–C1–C2–C7 7.3(6), O2–C4–C3–C8 12.5(6).

² The substitution of one Cl atom by one $-\text{CN}$ group increases the enthalpy of sublimation by $\sim 5.5 \text{ kJ mol}^{-1}$ (See Table S1a, Entries 3 and 4) while the substitution of four Cl atoms by four $-\text{CN}$ groups results in an increase of $\sim 18\text{--}41 \text{ kJ mol}^{-1}$ (Table S1a, Entries 1, 2, 10, 11). Therefore, the increase in sublimation enthalpy for each substitution of one Cl atom by one $-\text{CN}$ group is $\sim 5\text{--}10 \text{ kJ mol}^{-1}$; hence the enthalpy of sublimation for **1** is estimated as $110\text{--}120 \text{ kJ mol}^{-1}$. We will use the latter value throughout, so that the resulting solid state thermodynamic estimates from Born-Haber cycles will be a lower limit.

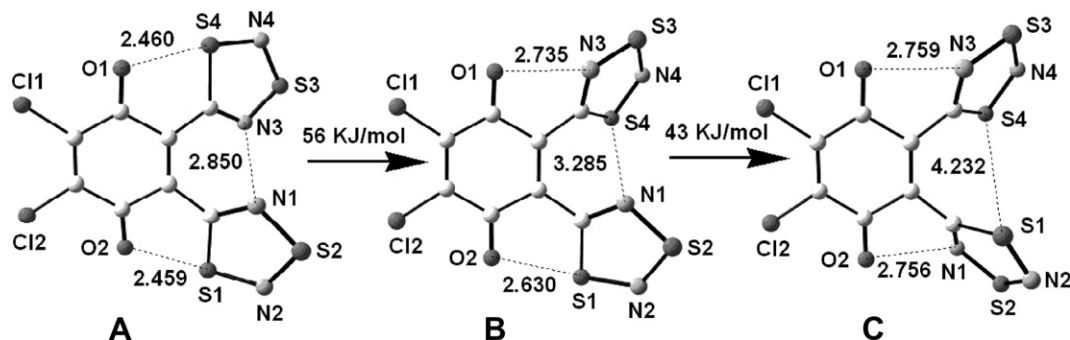
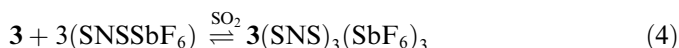
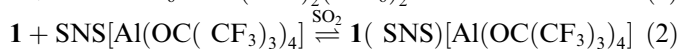
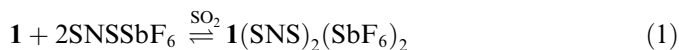


Fig. 3. The estimated relative energy difference for the three rotational isomers (A–C) for $1(\text{SNS})_2^{2+}$ based on the gas phase (MPW1PW91/6-31G*) calculated energies³.

approximated from the integration of the ^{13}C chemical shifts of similar substituted carbons and were consistently found to be ca. 1:2, even after most of the product ($1(\text{SNS})_2(\text{SbF}_6)_2 \cdot \text{SO}_2$) had crystallized or precipitated from the solution. After 7 days all SNSSbF_6 was consumed (^{14}N NMR), giving a mixture of products (the ratio of $1(\text{SNS})_2^{2+}$ and $1(\text{SNS})^+$ remained $\sim 2:1$, ^{13}C NMR) and a yellow-orange precipitate, assumed to be $1(\text{SNS})_2(\text{SbF}_6)_2 \cdot \text{SO}_2$. Thus the reaction of SNSSbF_6 and **1** gives $1(\text{SNS})_2(\text{SbF}_6)_2$ in essentially quantitative yield, on an NMR scale. On the other hand, the reaction of $\text{SNS}[\text{Al}(\text{OC}(\text{CF}_3)_3)_4]$ with **1** in a 1:1 stoichiometric ratio (Eq. (2)) followed by multinuclear NMR (^{13}C , ^{14}N , ^{19}F , ^{27}Al) resulted in the formation of only the monocycloaddition product $1(\text{SNS})^+$ and unreacted **1** and $\text{SNS}[\text{Al}(\text{OC}(\text{CF}_3)_3)_4]$ in solution after 3 weeks. An analogous reaction of SNSSbF_6 with the mono-nitrile **2** (Eq. (3)) provided $2(\text{SNS})^+$ in SO_2 solution as confirmed by ^{13}C (obs. (calc.) 192.8(190.8), 177.3 (173.8), 173.3 (168.6), 162.5 (160.3), 142.3 (155.6), 141.7 (150.2), 113.7 (114.3), 67.8 (73.2)) and ^{14}N NMR (Figure S21 and S22, respectively). The experimental ^{13}C NMR resonances of $2(\text{SNS})^+$ (as SbF_6^- salt) further simplifies and confirm the assignment of the ^{13}C NMR resonances for the monocycloaddition product $1(\text{SNS})^+$ as the $\text{Al}(\text{OC}(\text{CF}_3)_3)_4^-$ salt, and by comparison with calculated NMR tensors.



³ Both rotational isomers B and C optimize in the gas-phase to give rotational isomer A when no symmetry constraints are imposed (all other symmetries, C_s or C_2 are 2nd order or higher saddle points, by frequency analysis). We choose the following criteria to evaluate the relative energy difference between rotational isomers A–C (shown in Fig. 2): The first structure in the optimization steps to achieve the bond lengths, which are within 60% of the sum of the two “observed” mean van der Waals radii for the respective atom, (cf. C–C \AA 1.50 \AA , C–Cl \AA 1.75 \AA , C–N \AA 1.30 \AA , C–O \AA 1.24 \AA , C–S \AA 1.75 \AA , S–N \AA 1.70 \AA) as visualized in ChemCraft Version 1.5 [17a].

3.2. Cycloaddition chemistry of SNS^+ with **3**

The reverse electron demand cycloaddition of the Lewis acid SNS^+ with multiple bonds that act as Lewis bases is well established (the reaction rate is inversely proportional to the differences in the energies of the LUMO(SNS^+) and the HOMO(triple bond)) [1,3a], and therefore the cycloaddition of SNS^+ with **3** is expected to undergo a site selective cycloaddition at one of the four nitrile functionalities (HOMO), and not at the electron deficient $-\text{C}=\text{C}-$ bond [28]. In refluxing SO_2 solution, reaction of an excess of SNSSbF_6 (enough to afford the tetra-cycloaddition product) with **3** gave a mixture of the site selective cycloaddition products (1:1, 1:2 and 1:3 cycloaddition products, IR), which are less soluble, while the more soluble fraction contained starting materials (**3** and SNSSbF_6) and a small amount of unidentified cycloaddition products (IR). The mass balance did not fit the quantitative formation of $3(\text{SNS})_3(\text{SbF}_6)_3 \cdot \text{SO}_2$. A small scale experiment, performed at room temperature, gave colorless crystals of $3(\text{SNS})_3(\text{SbF}_6)_3 \cdot \text{SO}_2$ in moderate yield (40% isolated yield based on **3** and Eq. (4)). The structure of $3(\text{SNS})_3(\text{SbF}_6)_3 \cdot \text{SO}_2$ was determined by X-ray crystallography (Fig. 4, Section 3.3.2) and further characterized by IR and Raman microscopy (Figures S5 and S9, respectively).

3.3. X-ray crystallography

3.3.1. X-ray crystal structure of $1(\text{SNS})_2(\text{SbF}_6)_2 \cdot \text{SO}_2$

$1(\text{SNS})_2^{2+}$ given in Fig. 2, is the first X-ray crystallographic structure determination of an *ortho* bis-1,3,2,4-dithiadiazolylium cation, and only the second example to be prepared and characterized (cf. $7(\text{SNS})_2^{2+}$) [8]. In the solid state, the dicationic species are well separated from each other and make a number of weak contacts with six surrounding SbF_6^- anions (structural parameters of SbF_6^- anion given in Figures S11 and S13 in the supplemental material). $\text{S}^{\delta+} \cdots \text{F}^{\delta-}$ contacts fall in the range 2.986(3)–3.466(5) \AA . The molecules of SO_2 ($d(\text{S}-\text{O}) = 1.405(4)$ and $1.415(4)$ \AA , $\angle\text{O}-\text{S}-\text{O} = 118.3(3)^\circ$) are shorter than those found in the gas-phase ($d(\text{S}-\text{O}) = 1.431(2)$ \AA , $\angle\text{O}-\text{S}-\text{O} = 118.5(10)^\circ$) [29] and the solid state ($d(\text{S}-\text{O}) = 1.4297(4)$ \AA , $\angle\text{O}-\text{S}-$

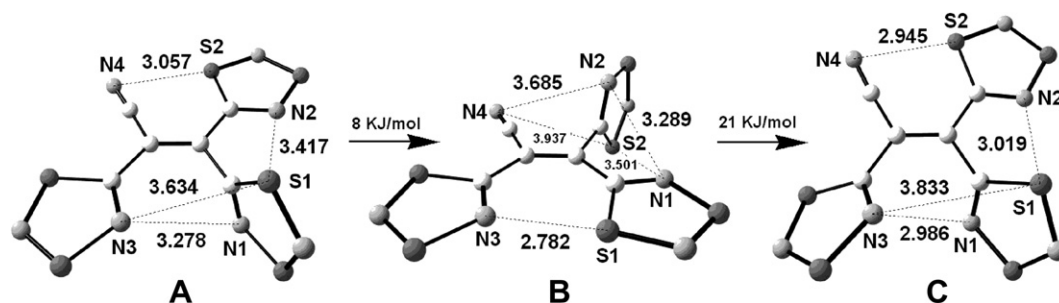
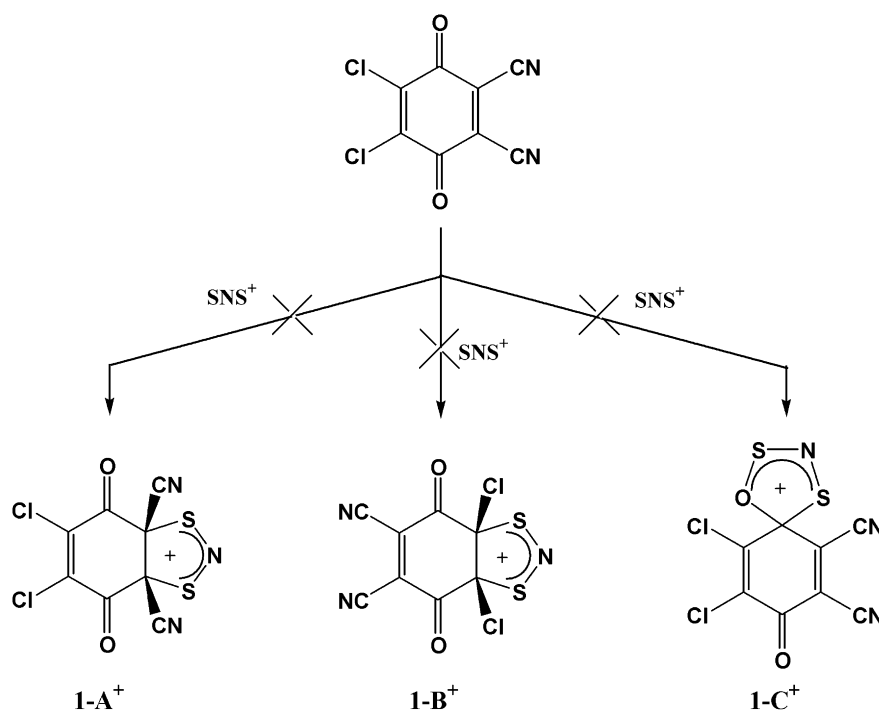


Fig. 5. The optimized gas-phase conformation of isomers A and B and the conformation corresponding to the actual X-ray structure, isomer C of $3(\text{SNS})_3^{3+}$ (the latter was a single point calculation).



Scheme 1.

$\angle\text{O-S-O} = 117.5(1)^\circ$ [17b,17c,17d]) of solvation, which is coordinated to both -CNSNS R2 and R3 rings ($\text{S}^{\delta+}\text{-O}^{\delta-}$, 3.073(3) and 3.113(4) Å) in a bridging motif (Figure S15, supplemental material). The $\text{S}^{\delta+}\text{-F}^{\delta-}$ and the $\text{S}^{\delta+}\text{-O}^{\delta-}$ interactions from the SO_2 molecules may account for the small distortion of isomer C from that of isomer A, calculated as the most stable conformation in the gas phase.

3.4. Energetics of the cycloaddition of SNS^+ with nitriles

3.4.1. Site selective cycloaddition of SNS^+ to **1**

The site selective cycloaddition of SNS^+ at the nitrile functionality of **1** is thermodynamically preferred ($>160 \text{ kJ mol}^{-1}$ in gas-phase and solution) relative to the other four unsaturated centers (two C=O and two C=C bonds), see Scheme 1 and Table 2 (entries 5–7). Typical 1,3-dipoles (e.g., diazoalkanes, nitrones) undergo cycloaddition reactions with quinones at the -C=C- bond or the C=O moieties [28]. The most common site of cycloaddition in **1** is at the NC-C=C-CN double bond [32]. How-

ever, the site selective cycloaddition of SNS^+ with **1** occurs at the nitrile functionalities exclusively. This is in accordance with previous results which showed that reactions of C=O and $\text{X}_2\text{-C=C-X}_2$ ($\text{X} = \text{F, Cl}$) with SNS^+ were likely thermodynamically and kinetically unfavorable [33].⁵

However, the reverse electron demand cycloaddition of SNS^+ with **1** ($\text{LUMO}(\text{SNS}^+) \text{-HOMO}(\text{C}\equiv\text{N})$) does not appear to proceed through the HOMO-LUMO interaction as found previously for other nitriles, since the HOMO

⁵ On the basis of a simplification of Klopman's equation, $\Delta E_{\text{MO}} = [\text{LUMO}_{\text{SNS}^+} - \text{HOMO}_{\text{AB}}]^{-1}$ ($\text{AB} = \text{unsaturated bond (ie. C=C, C=C, C}\equiv\text{N)}$) found the kinetic barriers should be small ($E_{\text{kinetic}} \propto (E_{\text{MO}})^{-1}$). However, a charge term (ΔE_{CH}) and for the electrophilic $\text{CF}_2\text{-C=C-CF}_2$ is dominant, and the reaction is kinetically unfavorable ($\Delta E'_{\text{MO}} = \Delta E_{\text{MO}} + \Delta E_{\text{CH}}$). A simple thermodynamic model of bonds formed minus bonds broken suggested the reactions were possibly thermodynamically unfavorable. Moreover, the reaction of SNS^+ with a variety of $\text{R}_2\text{C=O}$ ($\text{R} = \text{F, CH}_3, \text{'Bu, CF}(\text{CF}_3)_2$) and $\text{X}_2\text{C-C=C-CX}_2$ ($\text{X} = \text{F, Cl}$) did not occur experimentally.

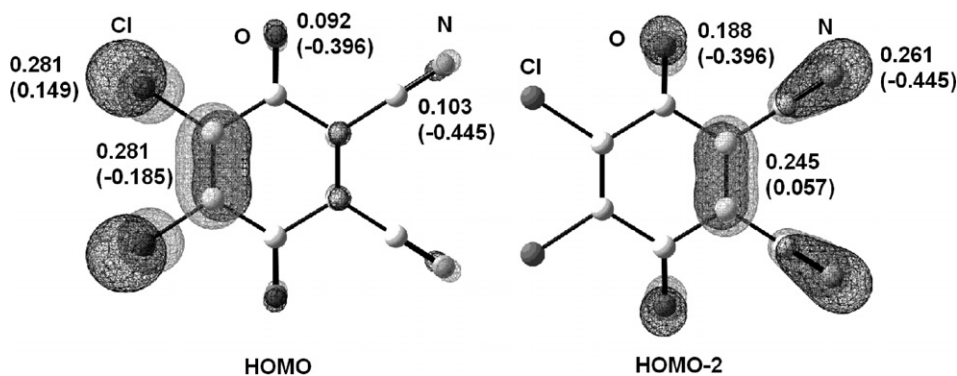


Fig. 6. Atomic orbital coefficients of HOMO and HOMO-2 of **1** calculated at the MPW1PW91/6-31G* level of theory. Mulliken charges are given in brackets.

(MO 56, $E = -0.3191$ a.u.) of **1** is largely located on the Cl–C=C–Cl portion of **1** (Fig. 6). Instead, the reaction is most likely to proceed by donation of electron density from a lower lying filled molecular orbital of **1** (HOMO-2; MO 54, $E = -0.3474$ a.u.) of correct symmetry into the LUMO of SNS⁺. This discrepancy can be rationalized given the larger atomic coefficients of the HOMO-2 at the nitrogen atoms (0.261 versus 0.103 a.u. of the HOMO), because the large coefficients aids the more pronounced charge transfer to the LUMO of SNS⁺.

The proximity of the electronegative oxygen to the nitrile group may provide an ideal in-plane electrostatic interaction that facilitates the cycloaddition of SNS⁺ with the nitrile functionality (–CN), similar to that proposed for the electrostatic interaction of SNS⁺ with the nitrogen in the 4-position of the 1,3,2,4-dithiadiazolium ring [9a,9b]. Kinetic factors involving atomic orbital coefficients, charges, and steric interactions have previously been suggested to account for the formation of a number of di- and tri-cycloaddition products of SNSMF₆ (M = As, Sb) with the corresponding nitriles [3a,3f], despite the expectation that additional cycloadditions would become increasingly less kinetically favorable. However, experimentally these reactions typically proceed to give the multiple cycloaddition products in essentially quantitative yield [5e,8,9].

Recently, the cycloaddition reaction of SNSMF₆ (M = As, Sb) with **11** and **12** has been shown to predominantly give the corresponding dicycloaddition products **11**(SNS)₂²⁺ and **12**(SNS)₂²⁺, respectively [10]. It was suggested that the reactions were under thermodynamic rather than kinetic control, since no preference for the second cycloaddition was found when the transition states were examined in the gas-phase by DFT quantum chemical calculations, although experimentally kinetic factors were not completely ruled out. Similar to the reaction of **1** and two equivalents of SNS⁺ reported herein, mixtures of both mono- (e.g., **11**(SNS)⁺ and **12**(SNS)⁺) and di-cycloaddition products (e.g., **11**(SNS)₂²⁺ and **12**(SNS)₂²⁺) were observed by ¹³C NMR, but could not be separated and isolated. However, in the case of **11**, a

few crystals of **11**(SNS)⁺ were obtained and the X-ray crystal structure determined [10]. This implies that under certain conditions (e.g., using a large excess of dinitrile) the mono-cycloaddition product could be isolated as the predominate product.⁶ We note that attempts to prepare mono- cycloaddition product, **6**(SNS)⁺, from SNS⁺ and a 10-fold excess of **6** were unsuccessful and yielded the di- cycloaddition, **6**(SNS)₂²⁺ in 97% yield (Table 3). This observation was originally explained by kinetic factors [3f,9b], but more recently, we account for this observation by the gain in lattice enthalpy of the 1:2 salts relative to twice that of the 1:1 salts and the low solubility of the di-cycloaddition product, **6**(SNS)₂(AsF₆)₂ in SO₂. Thus, given the similarity in ionic volumes for the anions AsF₆[−] ($V = 0.110$ nm³) and SbF₆[−] ($V = 0.121$ nm³), Fig. 2, and the solubility of their respective salts, similar trends are expected to be observed for both salts.

3.4.2. Thermodynamic estimates of the cycloaddition of SNSM₆F₆ with **1** and **3**

In order to determine the relative trends in the reactivity of these systems we investigated the thermodynamics in the gas phase, solution (SO₂ and CH₂Cl₂) and solid state (Table 2). The first cycloaddition of SNS⁺ to **1** is favorable in the gas-phase (Table 2, Entry 1, -159 kJ mol^{−1}), while the second is unfavorable (Table 2, Entry 2, $+109$ kJ mol^{−1}). In SO₂ solution both the first and second cycloaddition of SNS⁺ with **1** are favorable by -103 and -63 kJ mol^{−1}, respectively, with similar values obtained for CH₂Cl₂ (Table 2). The free energies (ΔG) in SO₂ solution also indicate that both the first and second cycloaddition should be favorable, in accordance with the observed experimental results (NMR, see Section 3.1) in solution. However, the situation in CH₂Cl₂ solution may only favor the first cycloaddition since ΔG for the second cycloaddition is $+1$ kJ mol^{−1} (see Table 2, Entry 1).

⁶ In the case of the cycloaddition of one equivalent of SNSM₆F₆ with a four fold excess of the dinitrile NC–C₄F₈–CN (kinetic conditions) the monocycloaddition product (NC–C₄F₈–CNSNS) was isolated in good yield. K.V. Shuvaev and J. Passmore, unpublished results.

Table 3
Compilation of experimental results for the cycloaddition of SNSMF₆ (M = As, Sb) with multifunctional nitriles (Chart 1)

Compound ^a	Apparent reaction time	Temperature (°C)	Yield (%)	Identification/characterization ^{b,c}	Reference
1 (SNS) ₂ ²⁺	7 d	60	85	EA, IR, Raman, NMR, X-ray	this work
3 (SNS) ₃ ³⁺	12 d	25	44	IR, Raman, X-ray	this work
4 (SNS)	1.5 h	25	72	EA, IR, CV, NMR, MS, X-ray	[9a]
4 (SNS) ₂ ⁺	16 h	25	59	EA, IR, CV	[9a]
4 (SNS) ₃ ²⁺	16 h	25	84	EA, IR, UV-Vis, CV, X-ray	[9a]
5 (SNS) ⁺	20 h	25	96	IR, NMR, X-ray	[9b]
5 (SNS) ₂ ²⁺	10 w	45	76	EA, IR, NMR, X-ray	[9b,3f]
6 (SNS) ₂ ²⁺	5 d	50	97	EA, IR, Raman, NMR, MS, X-ray	[9b] ^d , [3f]
7 (SNS) ₂ ²⁺	18 h	25	75	EA, IR, NMR	[8]
8 (SNS) ₂ ²⁺	18 h	25	85	EA, IR, NMR	[8]
9 (SNS) ₂ ^{2+e}	18 h	25	92	EA, IR, CV, NMR, MS, X-ray	[8]
10 (SNS) ₃ ³⁺	5 d	25	70	EA, IR, NMR	[5e]
11 (SNS) ⁺	3 w	60	N/A ^f	NMR, Raman, IR, X-ray	[10]
11 (SNS) ₂ ²⁺	2 w	60	74	EA, IR, Raman, NMR, X-ray	[10]
12 (SNS) ^{†g}	3 d	60	90	IR, NMR, X-ray	[10]

^a The AsF₆⁻ salt unless otherwise noted.

^b Some abbreviations: EA = elemental analysis, CV = cyclic voltammetry, MS = mass spectrum.

^c ¹H and/or, ¹³C and/or, ¹⁴N NMR.

^d Trace of 1:1 monocycloaddition product might have been present, IR.

^e Other salts prepared included for **9**(SNS)₂²⁺: Cl⁻, Br⁻, S₃N₂⁻ and SbCl₆⁻ and for **10**(SNS)₃³⁺ the Cl⁻ salt.

^f Only a few crystals isolated and identified by X-ray crystallography, while in solution the 1:1 product is identified by ¹³C- and ¹⁴N NMR.

^g The SbF₆⁻ salt was prepared; Also, the 1:1 product was identified in solution by ¹³C- and ¹⁴N NMR.



In both the gas-phase and solution (SO₂ and CH₂Cl₂) the monocycloaddition product **1**(SNS)⁺ is stable with respect to dissociation to SNS⁺ and **1** (Eq. (5)) and disproportionation to **1**(SNS)₂²⁺ and **1** (Eq. (6)). The situation is reversed in the solid state where the difference between the lattice enthalpy gain for the resulting 1:2 salt **1**(SNS)₂(SbF₆)₂ (*U*_{pot} = 1322 kJ mol⁻¹) and the 1:1 salt for **1**(SNS)(SbF₆) (*U*_{pot} = 419 kJ mol⁻¹ × 2) exceeds the unfavorable gas-phase term for the second cycloaddition (see Table 2, Entry 2). Therefore, in the solid state the disproportionation reaction according to Eq. (6) is thermodynamically favored (ca. -335 kJ mol⁻¹; see Table 2, Entry 4).

In the case of **3**, only the first cycloaddition is favorable in the gas-phase, while in SO₂ solution the first three cycloadditions are favorable (-82, -71, -117 kJ mol⁻¹, respectively, Table 2, Entries 9–11). The lattice potential energy for **3**(SNS)₃(SbF₆)₃ must be large (*U*_{pot} ≥ -2100 kJ mol⁻¹) to overcome the sum of the gas-phase terms for each of the three cycloadditions (+410 kJ mol⁻¹), heat of sublimation of **3** (+82 kJ mol⁻¹) [34] and three times the lattice enthalpy of SNSbF₆ (-525 kJ mol⁻¹). The formation of the 1:1 salt, **3**(SNS)(SbF₆), is unfavorable in the solid state with respect to **3** and SNSbF₆ (+65 kJ mol⁻¹, Table 2, Entry 9). The disproportionation of two **3**(SNS)(SbF₆) to **3**(SNS)₂(SbF₆)₂ and **3** is favorable (-269 kJ mol⁻¹, Table 2, Entry 13) largely due to the gain in the lattice potential energy of the 1:2 salt with respect to twice that of the 1:1 salt. This is similar to the energetics of **1**.

3.4.3. Thermodynamics estimates of the cycloaddition of SNS[Al(OC(CF₃)₃)₄] with **1** and kinetic considerations

By the VBT estimates the formation of the 1:1 cycloaddition product containing the large (*V* = 0.758 nm³) weakly coordinating anion Al(OC(CF₃)₃)₄⁻ is favorable in the solid state ($\Delta H_{\text{rxn}} = -17 \text{ kJ mol}^{-1}$; see Table 2, Entry 1). However, the second cycloaddition in SO₂ solution is favorable (Table 2, Entry 1), and therefore the 1:2 cycloaddition product, **1**(SNS)₂²⁺ should also be observable in solution. Yet, experimentally only the 1:1 cycloaddition product, **1**(SNS)⁺ is observed, although the 1:2 product could be present, but still not observed by ¹³C NMR if in low concentration. Furthermore, reaction (Eq. (2)) at 40 °C for 16 days in SO₂ solution had little effect on the nature of the reaction products (little change in the relative ratio of the integrations in the ¹⁴N NMR for the peaks of **1**(SNS)⁺, **1** and SNS⁺, in the time frame of 4–16 days). This suggests that there might be ion pairing between Al(OC(CF₃)₃)₄⁻ and SNS⁺, which has previously been suggested for the SbCl₆⁻ and AlCl₄⁻ salts of SNS⁺, both of which failed to undergo clean cycloaddition chemistries [35]. Tight ion pair formation has been suggested [36] in the observed decomposition of the Al(OC(CF₃)₃)₄⁻ anion with highly electrophilic species, e.g., P₂I₃⁺. Ion-pair formation could decrease the rate of reaction of the cycloaddition reaction (a kinetic effect) and also affect the free energies (ΔG) of the second cycloaddition in solution. Our estimates of the thermodynamics imply that formation of **1**(SNS)₂[Al(OC(CF₃)₃)₄⁻]₂ is also favorable in the solid state, but surprisingly, this product was not observed. **1**(SNS)₂[Al(OC(CF₃)₃)₄⁻]₂, if formed, would likely be very soluble, in contrast to **1**(SNS)₂(SbF₆)₂ · SO₂, which is only moderately soluble in SO₂ solution. Thus removal of **1**(SNS)₂²⁺ from the solution drives the equilibrium,

(Eq. (1)) to the right side in the case of SbF_6^- . Alternatively, it is also possible that the estimates of lattice potential energies of the 1:2 $\text{Al}(\text{OC}(\text{CF}_3)_3)_4^-$ salts by the VBT equations with the current parameters of Jenkins et al may not be appropriate and may need further fine tuning to fit salts of very large anions (like $\text{Al}(\text{OC}(\text{CF}_3)_3)_4^-$ as well as dications containing separated positive charge centers (i.e., large spacer group). We also note that as far as we are aware, no 1:2 salts ($\text{Dication}[\text{Al}(\text{OR}_f)_4]_2^+$, where $R_f = \text{CH}(\text{CF}_3)_2$, $\text{C}(\text{CF}_3)_3$, $\text{C}(\text{CF}_3)_2(\text{C}_6\text{F}_5)$) have yet been reported in the literature [37b].

3.4.4. Accounting for the experimental observations for the cycloaddition of SNSMF_6 ($M = \text{As}, \text{Sb}$) with other multifunctional nitriles

We have also estimated the energies of the reactions of SNS^+ in the gas phase, solution and solid phase, for the multifunctional nitriles shown in Chart 1 that have been

investigated experimentally [5e,6,8,9] and a compilation of experimental results are given in Table 3. The corresponding thermodynamic estimates are given in Table 4.

In these experiments, it was observed that the cycloaddition of SNSMF_6 ($M = \text{As}, \text{Sb}$) with compounds containing two or more unsaturated centers results in the transformation of every nitrile group into a 1,3,2,4-dithiadiazolylium moiety without identification of the intermediate 1:1 cycloaddition products (Table 4). Only three known cases have been reported where the intermediate 1:1 cycloaddition product have been identified or isolated in the solid state [9,10]. Based on our thermodynamic approach, we show that the first cycloaddition is favorable in the gas-phase in all cases for the multifunctional nitriles 4–10, while the second is unfavorable in the gas-phase [37] (for tricyanomethide $(\text{C}(\text{CN})_3)^-$, 4, the unfavorable tri-cycloaddition product is $4(\text{SNS})_3^{2+}$) [9a], Table 4. In solution, the enthalpy (ΔH) and free energy changes (ΔG) for both the

Table 4
Calculated gas-phase and solution enthalpies (ΔH), solution Gibbs free energies (ΔG) and solid state estimates for multifunctional nitriles, 4–10 (Chart 1)

Entry	From Chart 1	Gas phase ^a	$X^- = [\text{SbF}_6^-]$ solid	$X^- = [\text{Al}]^-$ solid	SO_2 solution	
		ΔH	ΔH^b	ΔH^b	ΔH	ΔG^c
1	$4(\text{g}) + \text{SNS}^+(\text{g}) \rightarrow 4(\text{SNS})(\text{g})$	-578			-556	-136
2	$4(\text{g}) + 2\text{SNS}^+(\text{g}) \rightarrow 4(\text{SNS})_2^+(\text{g})^d$	-795			-222	-98
	$\text{K}[4](\text{s}) + 2\text{SNSX}(\text{s}) \rightarrow 4(\text{SNS})_2\text{X}(\text{s}) + \text{KX}(\text{s})$		-148	-168		
3	$4(\text{SNS})_2^+(\text{g}) + \text{SNS}^+(\text{g}) \rightarrow 4(\text{SNS})_3^{2+}(\text{g})$	+51			-124	-79
	$4(\text{SNS})_2\text{X}(\text{s}) + \text{SNSX}(\text{s}) \rightarrow 4(\text{SNS})_3(\text{X})_2(\text{s})$		-868	-637		
4	$5(\text{g}) + \text{SNS}^+(\text{g}) \rightarrow 5(\text{SNS})^+(\text{g})$	-246			-243	-206
	$5(\text{s}) + \text{SNSX}(\text{s}) \rightarrow 5(\text{SNS})\text{X}(\text{s})$		-165	-197		
5	$5(\text{SNS})^+(\text{g}) + \text{SNS}^+(\text{g}) \rightarrow 5(\text{SNS})_2^{2+}(\text{g})$	+178			-64	-14
	$5(\text{SNS})\text{X}(\text{s}) + \text{SNSX}(\text{s}) \rightarrow 5(\text{SNS})_2(\text{X})_2(\text{s})$		-252	-156		
6	$6(\text{g}) + \text{SNS}^+(\text{g}) \rightarrow 6(\text{SNS})^+(\text{g})$	-75			-74	-36
	$6(\text{s}) + \text{SNSX}(\text{s}) \rightarrow 6(\text{SNS})\text{X}(\text{s})$		-19	-48		
7	$6(\text{SNS})^+(\text{g}) + \text{SNS}^+(\text{g}) \rightarrow 6(\text{SNS})_2^{2+}(\text{g})$	+165			-78	-36
	$6(\text{SNS})\text{X}(\text{s}) + \text{SNSX}(\text{s}) \rightarrow 6(\text{SNS})_2(\text{X})_2(\text{s})$		-270	-172		
8	$7(\text{g}) + \text{SNS}^+(\text{g}) \rightarrow 7(\text{SNS})^+(\text{g})$	-153			-91	-50
	$7(\text{s}) + \text{SNSX}(\text{s}) \rightarrow 7(\text{SNS})\text{X}(\text{s})$		+5	-52		
9	$7(\text{SNS})^+(\text{g}) + \text{SNS}^+(\text{g}) \rightarrow 7(\text{SNS})_2^{2+}(\text{g})$	+93			-60	-23
	$7(\text{SNS})\text{X}(\text{s}) + \text{SNSX}(\text{s}) \rightarrow 7(\text{SNS})_2(\text{X})_2(\text{s})$		-315	-240		
10	$8(\text{g}) + \text{SNS}^+(\text{g}) \rightarrow 8(\text{SNS})^+(\text{g})$	-152			-96	-57
	$8(\text{s}) + \text{SNSX}(\text{s}) \rightarrow 8(\text{SNS})\text{X}(\text{s})$		+9	-48		
11	$8(\text{SNS})^+(\text{g}) + \text{SNS}^+(\text{g}) \rightarrow 8(\text{SNS})_2^{2+}(\text{g})$	+50			-85	-46
	$8(\text{SNS})\text{X}(\text{s}) + \text{SNSX}(\text{s}) \rightarrow 8(\text{SNS})_2(\text{X})_2(\text{s})$		-358	-283		
12	$9(\text{g}) + \text{SNS}^+(\text{g}) \rightarrow 9(\text{SNS})^+(\text{g})$	-160			-97	-57
	$9(\text{s}) + \text{SNSX}(\text{s}) \rightarrow 9(\text{SNS})\text{X}(\text{s})$		+1	-56		
13	$9(\text{SNS})^+(\text{g}) + \text{SNS}^+(\text{g}) \rightarrow 9(\text{SNS})_2^{2+}(\text{g})$	+55			-83	-44
	$9(\text{SNS})\text{X}(\text{s}) + \text{SNSX}(\text{s}) \rightarrow 9(\text{SNS})_2(\text{X})_2(\text{s})$		-353	-278		
14	$10(\text{g}) + \text{SNS}^+(\text{g}) \rightarrow 10(\text{SNS})^+(\text{g})$	-137	Enthalpy of sublimation of 10 not known	Enthalpy of sublimation of 10 not known	-90	-52
15	$10(\text{SNS})^+(\text{rmg}) + \text{SNS}^+(\text{g}) \rightarrow 10(\text{SNS})_2^{2+}(\text{g})$	+78			-76	-38
	$10(\text{SNS})\text{X}(\text{s}) + \text{SNSX}(\text{s}) \rightarrow 10(\text{SNS})_2(\text{X})_2(\text{s})$		-323	-254		
16	$10(\text{SNS})_2^{2+} + \text{SNS}^+ \rightarrow 10(\text{SNS})_3^{3+}$	+266			-60	-28

^a Includes zero point energy (ZPE) correction.

^b Calculated from appropriate Born-Haber cycles, using the calculated gas phase values and the volume based thermodynamic (VBT) estimates of the lattice potential energies (see supplemental material for full details).

^c Including thermal correction to Gibbs free energy taken from the MPW1PW91/6-31G*(gas-phase) frequency calculations.

^d The solid state thermodynamics are based on the lattice enthalpy estimates (VBT method) where $U_{\text{pot}}[\text{K}(\text{C}(\text{CN})_3)] = 608 \text{ kJ mol}^{-1}$, $U_{\text{pot}}[\text{K}\text{SbF}_6] = 567 \text{ kJ mol}^{-1}$, $U_{\text{pot}}[\text{K}[\text{Al}]] = 364 \text{ kJ mol}^{-1}$.

first and second cycloaddition are negative, implying the reactions are favorable, while in the solid state, the gain in lattice enthalpy for the resulting 1:2 salt (dication and two mono-anions) compared to twice that of the 1:1 salt (mono-cation and mono-anion), is greater than the unfavorable gas-phase term [14]. Therefore, the situation for the other nitriles in all three phases is similar to that of **1** and **3** when SNSMF₆ (M = As, Sb) is used.

While the nature of the substituents (electron-withdrawing or donating) and size of the substituent and spacer groups affect the heats of vaporization and lattice enthalpy, they only slightly change the values of the reaction enthalpy (ΔH) for SNS⁺ with multifunctional nitriles in the solid state, but not the general trend. The substituents (electron-withdrawing or donating) may also affect the kinetics of the reverse electron demand cycloaddition reaction of SNS⁺, but in general the starting materials and the monocycloaddition products are typically soluble, while MF₆⁻ (M = As, Sb) salts of the dicycloaddition products are moderately to sparingly soluble. Thus, the dicycloaddition product, once formed, precipitates out of solution, shifting the equilibrium in solution towards the thermodynamically favored dicycloaddition product.

4. Conclusion

We have demonstrated that the cycloaddition chemistry of SNSSbF₆ with **1** and **3** is synthetically useful in the preparation of sulfur–nitrogen heterocyclic rings that are not readily available by other synthetic routes. The observed preference for the di- and tri-cycloaddition product can be rationalized by means of the DFT calculations in both the gas-phase and solution and the volume based thermodynamic (VBT) approach [14]. These simple thermodynamic models are useful in understanding of the experimental findings, as well as identifying future synthetic targets of interest.

The 1:2 cycloaddition product of SNSSbF₆ with **1** provides access to a new class of hybrid quinoidal-thiazyl systems, which can potentially serve as electron acceptors for charge transfer complexes and redox reactions. The readily reducible 1,3,2,4-dithiadiazolylium cations and quinoidal ring potentially provide access to a variety of oxidation states, which are mixed organic main group radicals that on their own may have interesting conductive and magnetic properties. These compounds are also of interest in the coordination chemistry of transition metals, e.g. as possible hybrid magnetic materials. Furthermore, the preparation of the tri-cycloaddition product **3**(SbF₆)₃³⁺ from SNS⁺ and **3** provided access to this very strong electron acceptor, which is a particularly interesting precursor for charge transfer complexes with interesting physical properties.

The first synthetic application of the cycloaddition chemistry of SNS⁺ with the weakly coordinating Al(OC(CF₃)₃)₄⁻ anion, led exclusively to the formation of the 1:1 cycloaddition product in solution. The preparation of the 1:1 cycloaddition product, **1**(SNS)(Al-

(OC(CF₃)₃)₄) in solution, and the predicted stability of the 1:1 salt in the solid state, in contrast to the SbF₆⁻ case, is an encouraging result which should allow the preparation of other 1:1 cycloaddition products with a free –CN moiety. Subsequent reduction of the monocycloaddition products would potentially provide access to new monoradicals of current interest and is currently under investigation. Ion-pair formation between SNS⁺ and the Al(OC(CF₃)₃)₄⁻ anion has been suggested to explain the inconsistency with our simple thermodynamic model, which predicted the 1:2 cycloaddition product, **1**(SNS)₂[Al(OC(CF₃)₃)₄]₂, to be stable in solution and the solid state, however, **1**(SNS)₂[Al(OC(CF₃)₃)₄]₂ was not experimentally observed. Further investigation of the cycloaddition chemistry of SNS[Al(OC(CF₃)₃)₄] is necessary to access the potential of this new SNS⁺ salt.

5. Supplemental material

Optimized geometries as atomic coordinates (*x,y,z*) and total energies for all calculated molecules in gas-phase and solution. Details of electrostatic and thermodynamic estimates, calculated GIAO tensors, FT-IR and Raman spectra. Structural parameters for the **1**(SNS)₂(SbF₆)₂·SO₂ and **3**(SNS)₃(SbF₆)₃·SO₂.

All multinuclear NMR (¹³C, ¹⁴N, ¹⁹F, ²⁷Al), FT-IR and Raman spectra and supporting details.

Acknowledgments

J.P. thanks Professor Anthony Downs for the memorable stay in his lab during a sabbatical leave and Jesus College Oxford for the 1996/97 Visiting Senior Research Fellowship. During this time a meeting with Don Jenkins subsequently led to development of the ‘volume based thermodynamic’ derivation of lattice enthalpies and other thermodynamic quantities that are successfully applied in this paper (Ref. [14] and <http://www.warwick.ac.uk/go/thermochemistry/>).

We thank the Natural Sciences and Engineering Research Council (NSERC) of Canada and University of New Brunswick for financial support. We would like to thank Dr. Carsten Knapp, Dr. Mikko Rautainen, for helpful discussions and Ms. Maria Correia for help with the experimental work.

Appendix A. Supplementary material

Supplementary data associated with this article can be found, in the online version, at [doi:10.1016/j.ica.2007.05.033](https://doi.org/10.1016/j.ica.2007.05.033).

References

- [1] (a) S. Parsons, J. Passmore, *Acc. Chem. Res.* 27 (1994) 101; (b) C.M. Aherne, A.J. Banister, T.G. Hibbert, A.W. Lake, J.M. Rawson, *Polyhedron* 16 (1997) 4239.

- [2] (a) T.S. Cameron, A. Mailman, J. Passmore, K.V. Shuvaev, *Inorg. Chem.* 44 (2005) 6524;
(b) C. Knapp, A. Mailman, G.B. Nikiforov, J. Passmore, J. Fluorsc. Chem. 127 (2006) 916.
- [3] (a) S. Parsons, J. Passmore, M.J. Schriver, X. Sun, *Inorg. Chem.* 30 (1991) 3342;
(b) J. Jacobs, S.E. Ulic, H. Willner, G. Schatte, J. Passmore, S.V. Sereda, T.S. Cameron, *Dalton Trans.* (1996) 383;
(c) G.K. MacLean, J. Passmore, M.N.S. Rao, M.J. Schriver, P.W. White, D. Bethell, R.S. Pilkington, L.H. Sutcliffe, *Dalton Trans.* (1985) 1405;
(d) S. Parsons, J. Passmore, X. Sun, M. Regitz, *Can. J. Chem.* 73 (1995) 1312;
(e) A.J. Banister, I. Lavender, S.E. Lawrence, J.M. Rawson, W. Clegg, *Chem. Comm.* (1994) 29;
(f) S. Parsons, J. Passmore, P.S. White, *Dalton Trans.* (1993) 1499.
- [4] (a) A. Apblett, T. Chivers, *Chem. Comm.* (1987) 1889;
(b) A. Apblett, T. Chivers, *Can. J. Chem.* 68 (1990) 650;
(c) R.T. Boere, R.G. Hicks, R.T. Oakley, *Inorg. Synth.* 31 (1997) 94.
- [5] (a) J. Passmore, X. Sun, *Inorg. Chem.* 35 (1996) 1313;
(b) J.M. Rawson, A.J. Banister, I. Lavender, *Adv. Heterocyclic Chem.* 62 (1995) 137;
(c) W.V.F. Brooks, N. Burford, J. Passmore, M.J. Schriver, L.H. Sutcliffe, *Chem. Comm.* (1987) 69;
(d) N. Burford, J. Passmore, M.J. Schriver, *Chem. Comm.* (1986) 140;
(e) C. Aherne, A.J. Banister, A.W. Luke, J.M. Rawson, R.J. Whitehead, *Dalton Trans.* (1992) 1277.
- [6] (a) A.J. Banister, I. Lavender, J. M Rawson, W. Clegg, B.K. Tanner, R.J. Whitehead, *Dalton Trans.* (1993) 1421;
(b) A.J. Banister, I. Lavender, J.M. Rawson, R.J. Whitehead, *Dalton Trans.* (1992) 1449;
(c) T.S. Cameron, M.T. Lemaire, J. Passmore, J.M. Rawson, K.V. Shuvaev, L.K. Thompson, *Inorg. Chem.* 44 (2005) 2576.
- [7] (a) G. Antorrena, S. Brownridge, T.S. Cameron, F. Palacio, S. Parsons, J. Passmore, L.K. Thompson, F. Zarlaida, *Can J. Chem.* 80 (2002) 1568;
(b) S. Brownridge, H. Du, S.A. Fairhurst, R.C. Haddon, H. Oberhammer, S. Parsons, J. Passmore, M.J. Schriver, L.H. Sutcliffe, N.P.C. Westwood, *Dalton Trans.* (2000) 3365;
(c) A. Alberola, R.J. Collins, S.M. Humphrey, R.J. Less, J.M. Rawson, *Inorg. Chem.* 45 (2006) 1903;
(d) H. Du, R.C. Haddon, I. Krossing, J.M. Rawson, J. Passmore, M.J. Schriver, *Chem. Comm.* (2002) 1836;
(e) J.M. Rawson, A. Alberola, A. Whalley, *J. Mater. Chem.* 16 (2006) 2560;
(f) K. Awaga, T. Tanaka, T. Shirai, M. Fujimori, Y. Suzuki, H. Yoshikawa, W. Fujita, *Bull. Chem. Soc. Jpn.* 79 (2006) 25.
- [8] A.J. Banister, J.M. Rawson, W. Clegg, S.L. Birkby, *Dalton Trans.* (1991) 1099.
- [9] (a) A.J. Banister, I. Lavender, J.M. Rawson, W. Clegg, *Dalton Trans.* (1992) 859;
(b) S. Parsons, J. Passmore, M.J. Schriver, P.S. White, *Chem. Comm.* (1991) 369.
- [10] T.S. Cameron, A. Decken, M. Gabriel, C. Knapp, *J. Passmore, Can. J. Chem.* 85 (2007) 96.
- [11] (a) A.J. Banister, N. Bricklebank, I. Lavender, J.M. Rawson, C.I. Christopher, B.K. Tanner, W. Clegg, M.R.J. Elsegood, F. Palacio, *Angew. Chem. Int. Ed.* 35 (1996) 2533;
(b) P.J. Langley, J.M. Rawson, J.N.B. Smith, M. Schuler, R. Bachmann, A. Schweiger, F. Palacio, G. Antorrena, G. Gescheidt, A. Quintel, P. Rechsteiner, J. Hulliger, *J. Mater. Chem.* 9 (1999) 1431;
(c) A. Alberola, R.J. less, F. Palacio, C.M. Pask, J.M. Rawson, *Molecules* 9 (2004) 771;
(d) N.G.R. Hearn, K.D. Hesp, M. Jennings, J.L. Korcok, K.E. Preuss, C.S. Smithson, *Polyhedron* 26 (2007) 2047;
, For related examples see(e) W. Kaim, M. Moscherosch, *Coord. Chem. Rev.* 129 (1994) 157.
- [12] A. Decken, A. Mailman, S. Mattar, J. Passmore, *Chem. Comm.* (2005) 2366.
- [13] See for example (a) K. Suzuki, M. Tomura, S. Tanaka, Y. Yamashita, *Tetrahedron Lett.* 41 (2000) 8359;
(b) E. Tsiperman, J.Y. Becker, V. Khodorkovsky, A. Shames, L. Shapiro, *Angew. Chem. Int. Ed.* 44 (2005) 4015;
(c) N. Martin, I. Perez, L. Sanchez, C. Seoane, *J. Org. Chem.* 62 (1997) 870;
(d) Y. Yamashita, K. Ono, S. Tanaka, K. Imaeda, H. Inokuchi, M. Sano, *Chem. Comm.* (1993) 1803;
(e) M.R. Bryce, E. Chinarro, A. Green, N. Martin, A.J. Moore, L. Sanchez, C. Seoane, *Synth. Metals* 86 (1997) 1857.
- [14] (a) H.D.B. Jenkins, H.K. Roobottom, J. Passmore, L. Glasser, *Inorg. Chem.* 38 (1999) 3609;
(b) L. Glasser, H.D.B. Jenkins, *Chem. Soc. Rev.* (2005) 866, and references therein;
(c) H.D. B Jenkins, J.F. Leibman, *Inorg. Chem.* 44 (2005) 6359;
(d) L. Glasser, *Inorg. Chem.* 34 (1995) 4935, and references therein;
(e) H.D.B. Jenkins, D. Tudela, *J. Chem. Ed.* 80 (2003) 1482;
(f) H.D.B. Jenkins, *J. Chem. Ed.* 82 (2005) 950;
(g) D.W.M. Hofmann, *Acta. Crystallogr., Sect. B* 57 (2002) 489;
(h) H.D.B. Jenkins, H.K. Roobottom, J. Passmore, *Inorg. Chem.* 42 (2003) 2886;
(i) M.S. Westwell, M.S. Searle, D.J. Wales, D.H. Williams, *J. Am. Chem. Soc.* 117 (1995) 5013.
- [15] H.D. Becker, *J. Org. Chem.* 34 (1969) 1203.
- [16] (a) M. Murchie, J. Passmore, *Inorg. Synth.* 27 (1988) 76;
(b) M.P. Murchie, R. Kapoor, J. Passmore, G. Schatte, T. Way, *Inorg. Synth.* 31 (1997) 102.
- [17] (a) G.A. Zhurko, D.A. Zhurko, ChemCraft Version 1.5 (Build 275), Tool for Treatment of the Chemical Data (<http://www.chemcraft-prog.com>); The IR and Raman were assigned by visualization of the calculated frequencies (MPWIPW91/6-31G* and scaling factor of 0.95 used for all frequencies) in ChemCraft Version 1.5* Asym = asymmetric; sym = symmetric, str = stretching, bend = bending mode, br = broad, sh = shoulder.;
(b) K. Nakamoto, in: *Infrared and Raman Spectra of Inorganic and Coordination Compounds*, fourth ed., Wiley, New York, USA, 1986, Gas-phase IR and Raman of sulfur dioxide;
(c) A. Anderson, M.C.W. Campbell, *J. Chem. Phys.* 67 (1977) 4300, Infrared and Raman of crystalline sulfur dioxide;
(d) R. Mews, E. Lork, P.G. Watson, B. Gortler, *Coord. Chem. Rev.* 197 (2000) 277, Coordination compounds containing SO₂ complexed to related transition metal cations via oxygen;
(e) G.M. Begun, A.C. Rutenberg, *Inorg. Chem.* 6 (1967) 2212;
(f) T. Birchall, P.A.W. Dean, R.J. Gillespie, *J. Chem. Soc. (A)* (1971) 1777;
(g) I. Krossing, A. Reisinger, *Eur. J. Inorg. Chem.* (2005) 1979.
- [18] (a) J. Passmore, M.J. Schriver, *Inorg. Chem.* 27 (1988) 2749;
(b) S. Brownridge, J. Passmore, X. Sun, *Can. J. Chem.* 76 (1998) 1220.
- [19] (a) SMART 5.054, Bruker AXS, Inc., Madison, Wisconsin, USA, 1999.;
(b) SAINT 6.45, Bruker AXS, Inc., Madison, Wisconsin, USA, 2003.;
(c) G. Sheldrick, Bruker AXS, Inc., Madison, Wisconsin, USA, 1997.
- [20] G.M. Sheldrick, SHELX-97 Programs for Crystal Structure Analysis (Release 97-2) Institut für Anorganische Chemie der Universität Göttingen, 1997.
- [21] K.Brandenburg, M. Brandt, DIAMOND 3.1, Crystal Impact, Bonn, Germany.
- [22] M.J. Frisch, G.W. Trucks, H.B. Schlegel, G.E. Scuseria, M.A. Robb, J.R. Cheeseman, J.A. Montgomery Jr., T. Vreven, K.N. Kudin, J.C. Burant, J.M. Millam, S.S. Iyengar, J. Tomasi, V. Barone, B. Mennucci, M. Cossi, G. Scalmani, N. Rega, G.A. Petersson, H. Nakatsuji, M. Hada, M. Ehara, K. Toyota, R. Fukuda, J. Hasegawa, M. Ishida, T. Nakajima, Y. Honda, O. Kitao, H. Nakai, M. Klene, X. Li, J.E. Knox, H.P. Hratchian, J.B. Cross, V. Bakken, C. Adamo, J. Jaramillo, R. Gomperts, R.E. Stratmann, O. Yazyev, A.J. Austin, R. Cammi, C. Pomelli, J.W. Ochterski, P.Y. Ayala, K. Morokuma, G.A.

- Voth, P. Salvador, J.J. Dannenberg, V.G. Zakrzewski, S. Dapprich, A.D. Daniels, M.C. Strain, O. Farkas, D.K. Malick, A.D. Rabuck, K. Raghavachari, J.B. Foresman, J.V. Ortiz, Q. Cui, A.G. Baboul, S. Clifford, J. Cioslowski, B.B. Stefanov, G. Liu, A. Liashenko, P. Piskorz, I. Komaromi, R.L. Martin, D.J. Fox, T. Keith, M.A. Al-Laham, C.Y. Peng, A. Nanayakkara, M. Challacombe, P.M.W. Gill, B. Johnson, W. Chen, M.W. Wong, C. Gonzalez, J.A. Pople, GAUSSIAN 03, Revision C. 02, Gaussian, Inc., Wallingford, CT, 2004.
- [23] (a) J.P. Perdew, K. Burke, M. Ernserhof, *Phys. Rev. Lett.* 77 (1996) 3865;
(b) J.P. Perdew, K. Burke, M. Ernserhof, *Phys. Rev. Lett.* 78 (1997) 1396;
(c) J.P. Perdew, M. Ernserhof, K. Burke, *J. Chem. Phys.* 105 (1996) 9982;
(d) C. Adamo, V. Barone, *J. Chem. Phys.* 110 (1999) 6158.
- [24] (a) C. Adamo, V. Barone, *J. Chem. Phys.* 108 (1998) 664;
(b) E. Cancès, B. Mennucci, J. Tomasi, *J. Chem. Phys.* 107 (1997) 3032;
(c) M. Cossi, V. Barone, B. Mennucci, J. Tomasi, *Chem. Phys. Lett.* 286 (1998) 253.
- [25] (a) J.F. Leiberman, in: J.F. Leiberman, A. Greenberg (Eds.), *Molecular Structure and Energetics*, vol. 3, VCH, Deerfield Beach, FL, 1986.
- [26] A.S. Coolidge, M.S. Coolidge, *J. Am. Chem. Soc.* 49 (1927) 100.
- [27] Some sharp and distinct, well resolved peaks in the IR spectrum (cm^{-1}) of $\mathbf{1}(\text{SNS})_2(\text{SbF}_6)_2 \cdot \text{SO}_2$: $\nu_{\text{sym}} \text{C}=\text{O}$ (1689s) and $\nu_{\text{assym}} \text{C}=\text{O}$ (1667s), $\nu \text{C}=\text{C}$ (1574s), $\nu \text{C}-\text{C}$ or SO_2 (1084s), $\nu_{\text{assym}} \text{S}-\text{N}$ (980w), $\nu_{\text{sym}} \text{SNS}$ (756w), $-\text{CNSNS}$ ring (447m) are distinct but unambiguous proof that the 1:1 salt, $\mathbf{1}(\text{SNS})\text{SbF}_6$, is not present in the solid state based on the experimental IR is difficult given the expected weak ν ($-\text{CN}$) in an IR spectrum or lack thereof. The calculated (MPW1PW91/6-31G⁺) IR for $\mathbf{1}$, $\mathbf{1}(\text{SNS})^+$ and $\mathbf{1}(\text{SNS})_2^{2+}$ are closely related as well.
- [28] (a) R. Huisgen, G. Mloston, E. Langhals, *Helv. Chim. Acta* 84 (2001) 1805;
(b) J.E. Franz, R.K. Howe, H.K. Pearl, *J. Org. Chem.* 41 (1976) 620;
(c) T. Oshima, H. Kitamura, T. Higashi, K. Kokubo, N. Seike, *J. Org. Chem.* 71 (2006) 2995;
(d) T. Hayakawa, K. Araki, S. Shiraishi, *Bull. Chem. Soc. Jpn.* 57 (1984) 2216.
- [29] A.H. Clark, B. Beagley, *Faraday Trans. Soc.* (1971) 2216.
- [30] A. Bondi, *J. Phys. Chem.* 68 (1964) 441.
- [31] G. Zanotti, R. Bardi, A. Del Pra, *Acta Crystallogr., Sect. B* 36 (1980) 168.
- [32] (a) T. Oshima, T. Nagai, *Bull. Chem. Soc. Jpn.* 59 (1986) 3865;
(b) S. Shiraishi, A. Ikeuchi, M. Seno, T. Asahara, *Bull. Chem. Soc. Jpn.* 51 (1978) 921;
(c) L.T. Scott, I. Erden, W.R. Brumsvold, T.H. Schultz, K.N. Houk, M.N. Paddon-Row, *J. Am. Chem. Soc.* 104 (1982) 3659;
(d) G.I. Fray, J.M. White, *Acta Crystallogr., Sect. C* 44 (1988) 1926.
- [33] M.J. Schriver, Ph.D. Thesis, University of New Brunswick, Canada, 1988.
- [34] R.H. Boyd, *J. Chem. Phys.* 38 (1963) 2524.
- [35] B. Ayres, A.J. Banister, P.D. Coates, M.I. Hanford, J.M. Rawson, C.E.F. Rickard, M.B. Hursthouse, K.M. Abdul Malik, M. Motevalli, *Dalton Trans.* (1992) 3097.
- [36] (a) M. Gonsior, I. Krossing, L. Muller, I. Raabe, M. Jansen, L. van Wullen, *Chem. Eur. J.* 8 (2002) 4475;
(b) I. Krossing, I. Raabe, *Angew. Chem. Int. Ed.* 43 (2004) 2066;
(c) I. Krossing, *Dalton Trans.* (2002) 500;
(d) M. Gonsior, I. Krossing, N. Mitzel, *Z. Anorg. Allg. Chem.* 628 (2002) 1821;
(e) H. Noth, A. Schlegel, J. Knizek, I. Krossing, W. Ponikwar, T. Seifort, *Chem. Eur. J.* 4 (1998) 2191.
- [37] (a) M.K. Scheller, R.N. Compton, L.S. Cederbaum, *Science* 270 (1995) 1160;
(b) D. Schröder, H. Schwarz, *J. Phys. Chem. A* 103 (1999) 7385;
(c) A. Dreuw, L.S. Cederbaum, *Chem. Rev.* 102 (2002) 181.